THE REPUBLIC OF TURKEY

BAHCESEHIR UNIVERSITY

STRUCTURED-LIGHT 3D SURFACE IMAGING SYSTEM

Master Thesis

WALEED ISMAEL

İSTANBUL, 2015

THE REPUBLIC OF TURKEY
BAHCESEHIR UNIVERSITY

NATRUAL AND APPLIED SCIENCES
DERPARTMANT OF COMPUTER ENGINEERING

STRUCTURED-LIGHT 3D SURFACE IMAGING

Master Thesis

WALEED ISMAEL

Supervisor: Assist. Prof. Dr. TARKAN AYDIN

İSTANBUL, 2015

THE REPUBLIC OF TURKEY
BAHCESEHIR UNIVERSITY

NATURAL AND APPLIED SCIENCES
DEPARTMENT OF COMPUTER ENGINEERING

Name of the thesis: Structured-Light 3D Surface Imaging
Name/Last Name of the Student: Waleed Ismael
Date of the Defense of Thesis:

The thesis has been approved by the Graduate School of Natural and Applied Sciences

Graduate School Director
Assoc. Prof. Dr. Nafiz ARICA
Signature

I certify that this thesis meets all the requirements as a thesis for the degree of Master of Arts.

Program Coordinator
Assist. Prof. Dr. Tarkan AYDIN
Signature

This is to certify that we have read this thesis and we find it fully adequate in scope, quality and content, as a thesis for the degree of Master of Arts.

Examining Committee Members	**Signature**
Thesis Supervisor Assist. Prof. Dr. Tarkan AYDIN	--------------------------------
Thesis Co-supervisor Assist. Prof. Dr. Cemal Okan Şakar	---------------------------------
Member Assist. Prof. Dr. Ali SIRMA	---------------------------------
Member None	--------------------------------

ACKNOWLEDGMENTS

I would like to express my deepest gratitude to my supervisor Assist. Prof. Ph.D. Tarkan AYDIN, for his advices, guidance, encouragements, and insight thoughts of this research. I also would like to thank my family for their help and support through my whole life. I would never have reached this level of education without their continuous inspiration and support.

İstanbul, 2015 Waleed ISMAEL

ABSTRACT

STRUCTURED-LIGHT 3D SURFACE IMAGING

WALEED ISMAEL

Department of Computer Engineering

Supervisor: Assist. Prof. Dr. Tarkan Aydin

September 2015, 64 pages

This thesis deals with two specific techniques of structured-light 3D surface imaging systems. 3D scanning technologies had major evolution in last few decades. One of the most commonly used 3D imaging techniques is global illumination, which requires to illuminate an object with certain patterns or uniquely labeled dots. Some of these techniques demands multiple pattern projections which requires the object to remain static until the process is done. In this paper we categorized and demonstrated most used 3D imaging techniques. Afterwards, we implemented two techniques (object illumination using binary coded patterns and phase-shifting patterns). Binary coded patterns and phase-shifting patterns are widely used methods in global illumination systems. They are simple, reliable and less costly comparing to other techniques. We selected these two techniques for the purpose of studying. We implemented and compared the outcome of 3D models and detected the advantages and disadvantages of each method.

Keywords: Image Acquisition, Phase-Shifting, Surface Imaging Systems, Stripe Indexing, Structured Light.

ÖZET

YAPILANDIRILMIŞ IŞIK İLE 3B YÜZEY GÖRÜNTÜLEME

WALEED ISMAEL

Bilgisayar Mühendisliği

Tez Danışmanı: Yard. Doç. Dr. Tarkan AYDIN

Eylül 2016, 64 sayfa

Bu tezde yapılandırılmış-ışık 3B yüzey görüntüleme sistemlerinde kullanılan iki özel teknik incelenmiştir. 3B tarama teknolojilerinde son yıllarda önemli gelişme sağladı. En sık kullanılan 3B görüntüleme tekniklerinden biri sahnenin yapılandırılmış ışık örüntüleri veya benzersiz etiketlerle aydınlatılasını içeren global tekniktir. Bu tekniklerden bazıları görüntüleme süreci boyunca sahnenin sabit kalmasını gerektiren birden fazla model projeksiyonlarını gerektirir. Bu çalışmada en çok kullanılan 3B görüntüleme teknikleri gösterildi. Daha sonra (ikili kodlanmış desen ve faz değiştiren kalıplarını kullanarak nesne aydınlatma) bilinen iki teknik uygulandı. İkili kodlanmış desen ve faz değiştiren desenler global aydınlatma sistemlerinde yaygın olarak kullanılan yöntemlerdir. Bunlar, basit, güvenilir ve diğer tekniklere göre daha az maliyetlidir. Çalışmada 3B görüntü sonuçlarını karşılaştırılmış ve her yöntemin faydaları ve dezavantajlarını tespit edilmiştir.

Anahtar Kelimeler: Görüntü Toplama, Faz-Shifting, Yüzey Görüntüleme Sistemleri, Şerit indeksleme, Yapısal Işık.

CONTENTS

FIGURES

ABBREVIATIONS

CAD	:	Computer Aided Design
CAM	:	Computer Aided Manufacturing
GWB	:	Gray, White, Black
PC	:	Portable Computer
PRA	:	Pseudo Random Array
PRBA	:	Pseudo Random Binary Array
WGB	:	White, Gray, Black
WHO	:	World Health Organization
XOR	:	Exclusive OR
2D	:	Two Dimensional
3D	:	Three Dimensional

1. INTRODUCTION

We often use cameras to precieve objects in real-world and yet cameras offer (2D) images which lack the information-depth of the objects. This substantial restriction weakens our capabilities to look upon and understand the details of the objects in our world. Accurate representation of objects has been in the lead of scientific concentration since for several decades. (2D) representations using rules and methods of projective and evocative geometry have been communal drill for centuries. It was from these (2D) demonstrations that (3D) three-dimensional information ought to be extracted. This mission required special education, hard preparation, talent and imagination. These days, techniques have been replaced by digital scanning which is accomplished using 3D imaging systems.

A “3D scanner” or “3D imaging” states to procedures to capture coordinates (x, y, z) from the scanned object. The inspiration of many application demands in variant of life necessities caused the past several eras to achieve tremendous advances in 3D scanning techniques. 3D scanning achieved great progress in many fields of science, examples in industrial and civil engineering, design processes, medical applications, and entertainments applications.

Figure 1.1: The Construction of Measurement Structure.

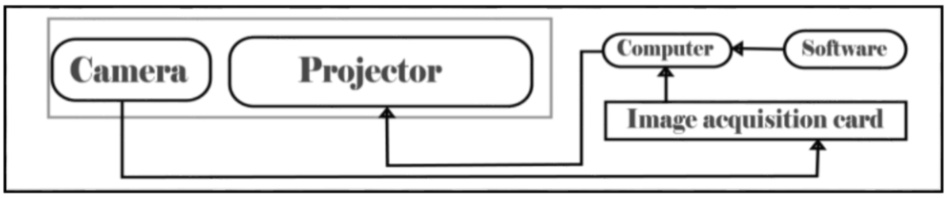

The construction of measurement structure is shown in Figure 1.1 the scanner has been planned nearby two communal electrical devices: a projector and a camera which combine a stereophonic image system. The projector is used to project light patterns on the targeted objective so it can be scanned. Instantaneously taken by the camera. As for the digital camera and the video projector are constitute a vision sensor. The devices are controlled by a software tool running on a standard computer, which products the sequence of arrays casted by the emitter and controls the camera. The software also contains other elements such as structure calibration, removing light bars, discovering communication, reform, demonstration, etc. As for the arranged patterns are driven by the computer.

Figure 1.2: Using Structured Light to Illuminate a 3D Object.

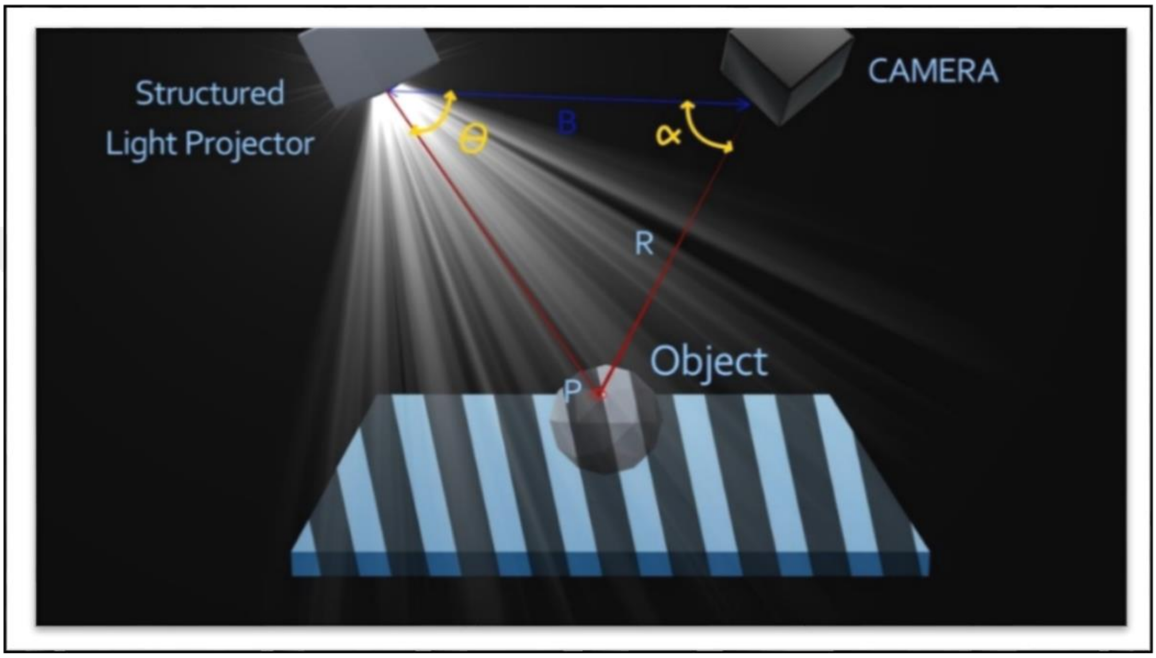

The most common methods of 3D surface scanning, is by using structured-light illumination striking a scene with special 2D patterns with varying forms based on different applications. As shown in Figure 1.2, a projector is a source of illumination of (2D) special patterns.

The digital signal $\{Iij = (i,j),\ i = 1,2,\ \dots,\ I, j = 1,2,\dots,J\}$ characterizes the concentration of each pixel on the structured-light. Where (I,j) represents the coordinates of the projected patterns (x,y). The objective of the cameras is to capture a 2D image of the object illuminated by the structured-light projector. While the surface of the object is non-planar, its surface distorts the patterns which are projected by structured-light and captured by the image sensors (cameras) in 2D image. And if the surface of the object is a planner without any dimensional variations, the projected patterns will be similar to the captured images by the sensors.

Studies concluded a triangular relationship between a structured-light, an imaging sensor, and a point on a surface of an object. And it is expressed by the principle below:

$$R = B\frac{sin(\Theta)}{sin(\alpha+\Theta)} \quad \mathbf{(1.1)}$$

The idea of this 3D imaging, based on the triangulation principle, is to separate a single light spot from the captured 2D image patterns on the surface of the targeted object. Many methods and schemes are submitted for this purpose as we here will discuss variety of these methods and determinate their pros and cons. We can classify those methods into two categories, multiple-shot technique and single-shot technique. Multiple-shot technique is recommended for scanning static objects which don’t require a specific acquisition time. And it can result a more accurate outcome. Otherwise if the targeted object is dynamic, then the single-shot technique should be applied to obtain an image of the object surface in an instance. As for single-shot technique, we classify it to three categories, using continues colored illumination patterns, using illumination with strips indexing, and illumination with grid indexing. To benefit from advantages or to avoid disadvantages of some techniques, we are able to combine and use multiple techniques to serve an exact purpose. Whatever the technique is being used, the key idea is to design patterns to illuminate globally and prevent any errors at the instant of capturing a light point on the targeted object. As the distance of the projector affects the frequency of the patterns, it is best to use high-frequency at long ranges and low-frequency at short range. Although using binary and sinusoidal codes in illuminated patterns fixes the issue of distance, for it is a combination of both high and low frequency patterns. Likewise, we can use tools of combinatorial calculations to design low-frequency patterns which are low enough to make them resistant to short range use.

This being said, there are more challenges facing Structured-light 3D surface imaging. The most significant ones are reflective and transparent surfaces. Reflective surface causes the light of one or more illuminated patterns to be reflected away from the camera or back to the projector. As for the transparent surfaces denies the light to be reflected to the camera. There for, it is highly recommended to overcoat the object with impermeable polish thin enough to prevent the light from passing through. Other problem is caused by translucent objects such as human tissue, Skin, and plants, because of the occurrence of sub-surface scattering. Another difficulty is scanning dynamic objects. Figure 1.3 shows the classification framework of most 3D imaging techniques.

Figure 1.3: Classification Structure of 3D Imaging Techniques.

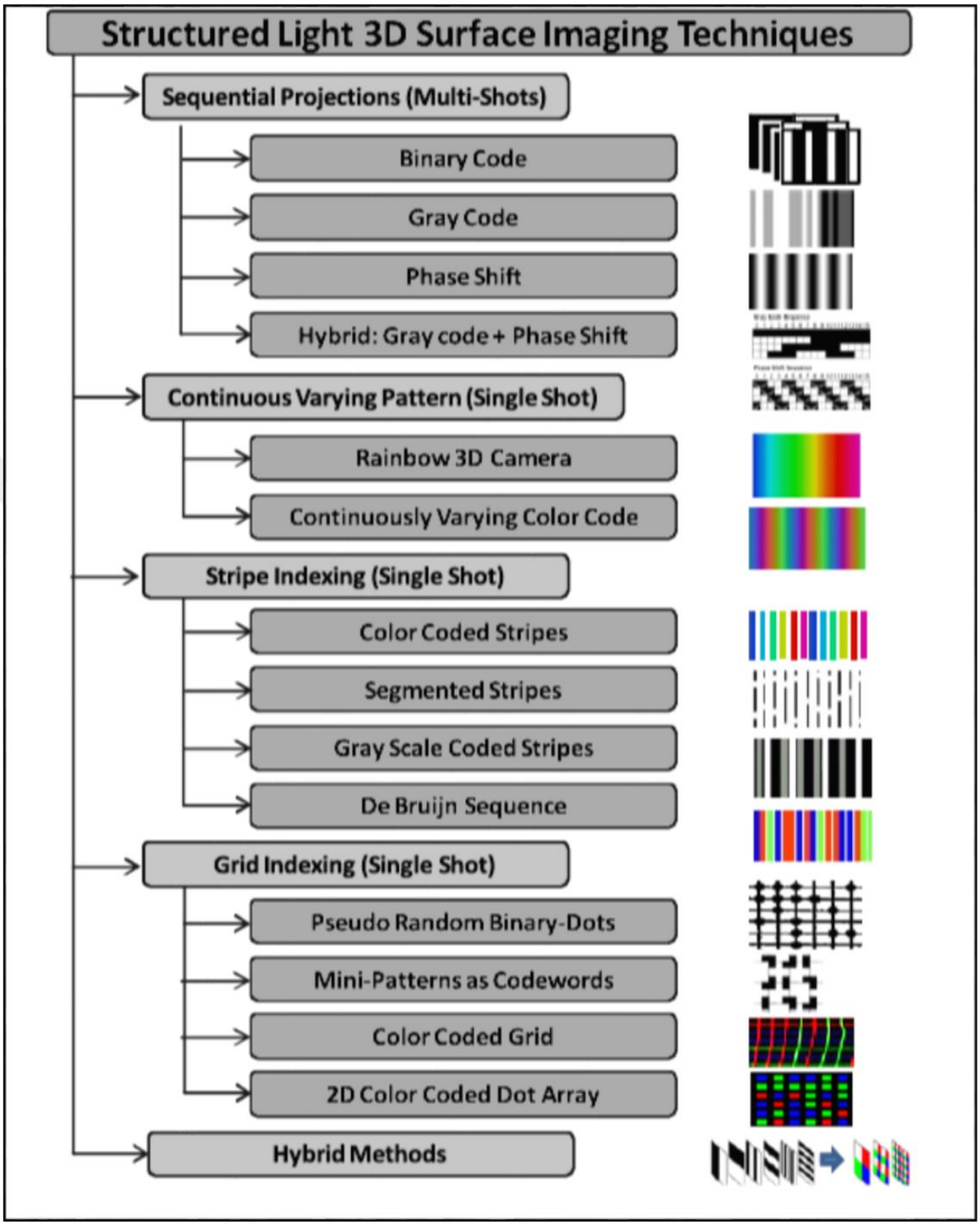

Source: Structured-Light 3D Surface Imaging: A Tutorial, By Jason Geng, 2011.

2. LITERATURE REVIEW

2.1 CONSECUTIVE PROJECTION METHODS

To understand the essential techniques and its principles of the majority of the methods can be used in 3D surface imaging, we will represent each technique as a tutorial to have the opportunity to cover them in this paper, for it is impossible to represent them all in details.

2.1.1 Coding With Binary Patterns

This method uses multiple sequined strikes of patterns to determine the coordinates of each point on an object. By using black and white bars in each pattern, we can assume N represents the number of patterns which can code 2^N stripes. Eventually the number of unique coded points will be 32 (2^5) Thus the (x, y, z) coordinates can be obtained using a triangulation-principle which will result the final fully framed 3D image (Ishii, 2015). Gray coding method is reliable. And because of the codes of the pixels are restricted to binaries only, has the potential to be less sensitive to the distortions of an object surface. However, the requirement of multiple sequences of patterns to have a high quality scanned image, the targeted object must remain static throughout the whole process which can be denied by some 3D applications. Figure 2.1 shows an example of the sequence of binary coded patterns which are projected for 3D imaging process.

Figure 2.1: Sequential Binary-Coded Pattern Projections for 3D Imaging.

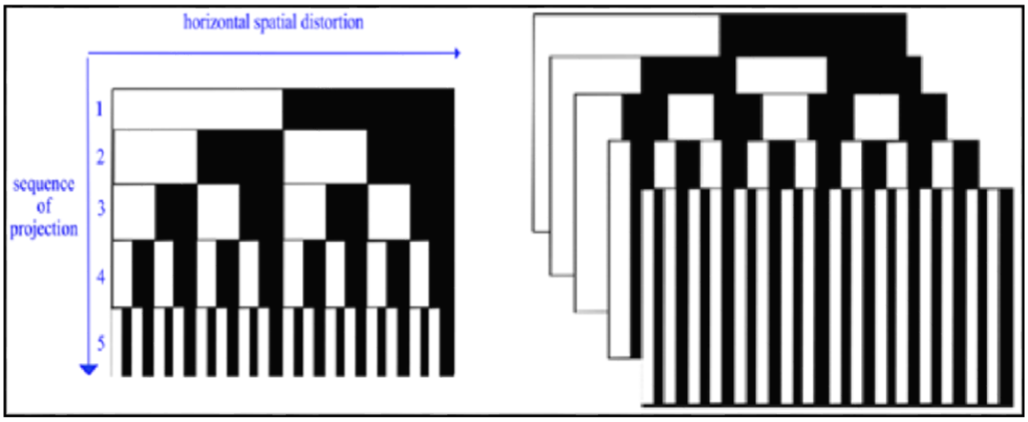

2.1.2 Patterns of Gray Level

Developing gray-level effectively resulted reducing the amount of projected patterns required to acquire a full framed 3D image with high quality. Instead of using two binary codes, we can assume M is the distinct levels of intensity which can produce unique codes for the projected patterns, and N patterns can code M^N Stripes. Comparing to binary patterns, if we want to produce 64 stripes, in binary patterns 6 projected patterns are needed to complete the sequence. As for the gray-level patterns, we can use 3 projected patterns to accomplish the same goal, assuming N=3 and M=4 (3^4) will result 64 stripes. The downside to this method is the overlap of the gray stripes with the white and black, as the number of strips increases the distance between the strips decreases, and the interference of the projector light colors will affect the outcome. Figure 2.2 illustrates an example of gray-level pattern sequence.

Figure 2.2: Gray-Level Coded Patterns Sequence.

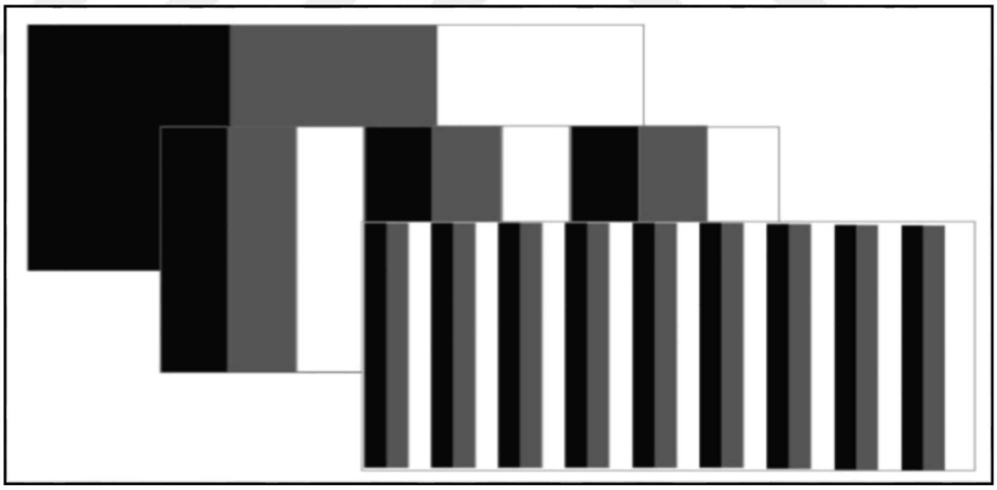

2.1.3 Phase shifting patterns

This method is a familiar border projection technique for 3D imaging of surface. A number of sinusoidal arrays are planned against the targeted object as shown in figure 2.3. We define the three projected border arrays of every concentrations for every pixel (x, y) as:

$$I1\ (x, y) = I0\ (x, y) + Imod\ (x, y) \cos\ (\varnothing\ (x, y) - \Theta), \quad \textbf{(2.1)}$$

$$I2\ (x, y) = I0\ (x, y) + Imod\ (x, y) \cos\ (\varnothing\ (x, y), \quad \textbf{(2.2)}$$

$$I3\ (x, y) = I0\ (x, y) + Imod\ (x, y) \cos\ (\varnothing\ (x, y) + \Theta). \quad \textbf{(2.3)}$$

Figure 2.3: An Example of Fringe Image and Phase-Shift with Three Projected Patterns.

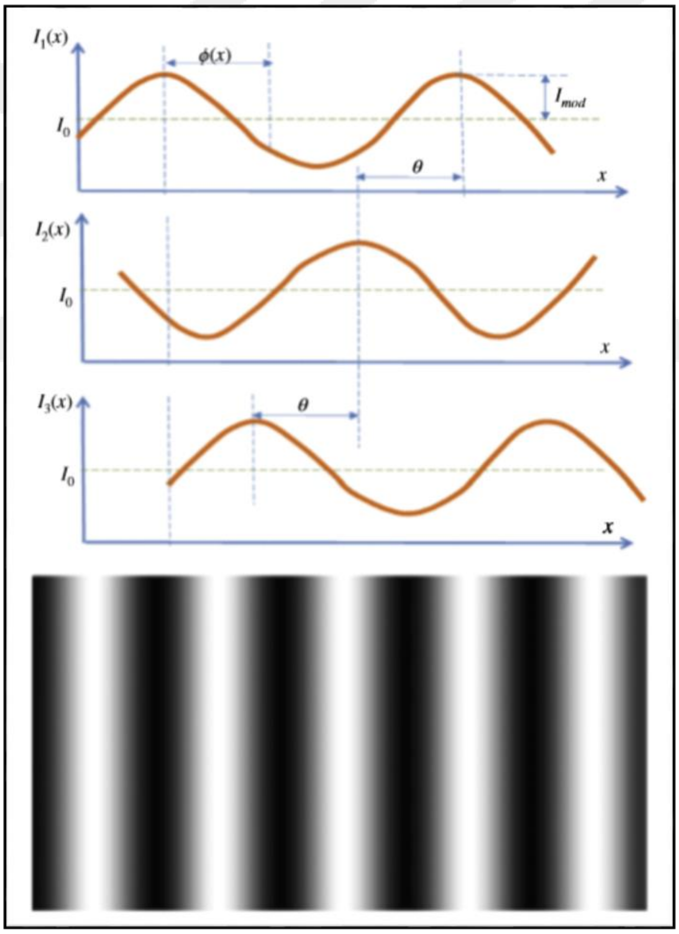

Source: Structured-Light 3D Surface Imaging: A Tutorial, By Jason Geng, 2011.

Where *I1(x, y), I2(x, y),* and *I3(x, y)* are the concentrations of three border arrays, *I0(x, y)* is the DC element, *Imod (x, y)* is the intonation motion largeness, Ø (x, y) is the phase, and ϴ is the continual phase-shift angle.

Unpacking of the phase is the procedure which transforms the phase which is packed to the utter phase. The phase info ϕ (x, y) is able to be recovered (unpacked) from the concentrations in the three border arrays:

$$\emptyset' = arctan\left[\sqrt{3}\frac{I_1(x,y)-I_3(x,y)}{2I_2(x,y)-I_1(x,y)-I_3(x,y)}\right]. \quad \textbf{(2.4)}$$

As shown in figure 2.4, the break of the function of the arch curve at 2π can be distant with the addition or subtraction the multiples of 2π on the Ø' (x, y) value:

$$\emptyset(x,y) = \emptyset'(x,y) + 2k\pi . \quad \textbf{(2.5)}$$

Figure 2.4: Sketch of Process of the Phase Unpacking.

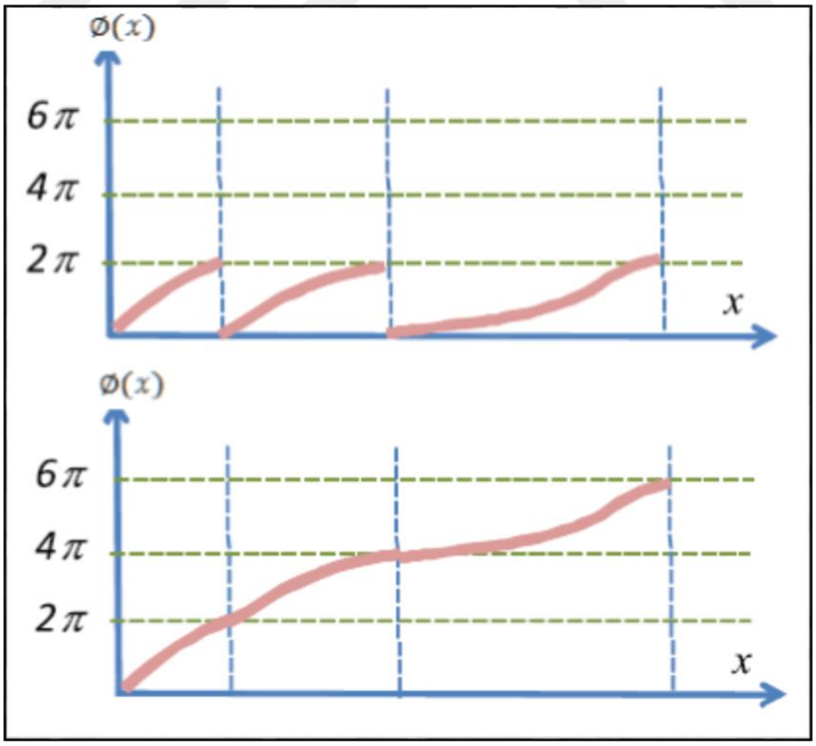

Source: Structured-Light 3D Surface Imaging: A Tutorial, By Jason Geng, 2011.

Figure 2.5: Calculating Z Distance Based On The Phase Rate.

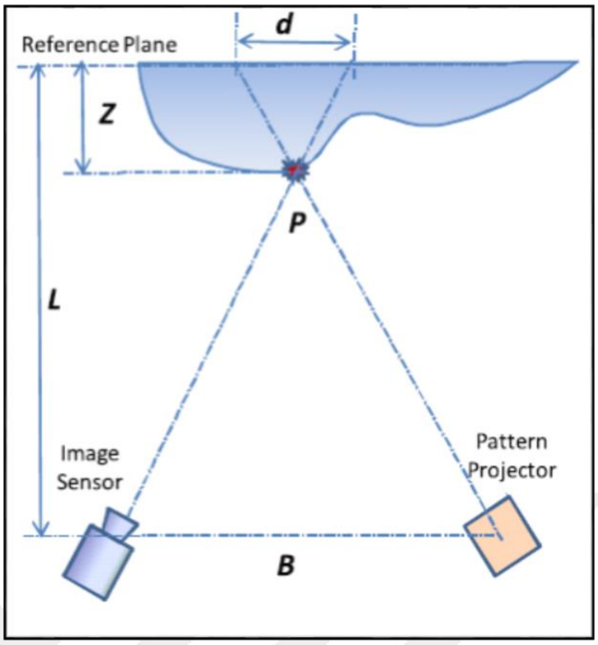

Source: Structured-Light 3D Surface Imaging: A Tutorial, By Jason Geng, 2011.

As for k is an integer signifying forecast period. We should note that unpacking techniques simply offer a comparative unpacking and do not resolve for the utter phase. According to the difference amongst the phase value from an orientation plane (Sagan, 2012) and dignified phase ∅ (x, y), we can calculate the 3D (x, y, z) coordinates. Figure 2.5 illustrates a simple example, as:

$$\frac{Z}{L-Z} = \frac{d}{B}, \quad or \quad Z = \frac{L-Z}{B} d. \qquad \textbf{(2.6)}$$

2.1.4 Hybrid Method: Phase Shift & Gray Coding

We already mentioned the two issues in phase shifting patters methods: the unpacking techniques simply delivers a virtual unpacking and will not resolve for the utter phase. The resulted method built on unpacking will correctly unpack two planes comparative to each other if the two planes have an incoherence of more than 2π. “Ambiguity” regularly is the term used for these difficulties, and the mixture of phase shift and gray code techniques can resolve these issues.

We illustrate a sample combining phase-shift with gray-code containing a sequence of 32 stripes in figure 2.6. As the gray coding method defines utter variety of the phase minus every opacity, however the phase-shift proposes sub-pixel resolution further than the number of bands delivered by the gray code [10, 12]. Yet, hybrid methods oblige a bigger quantity of the projected patterns and they do not provide themselves fit to 3D imaging of lively targeted objected.

Figure 2.6: Combining Gray-Code with Phase-Shift.

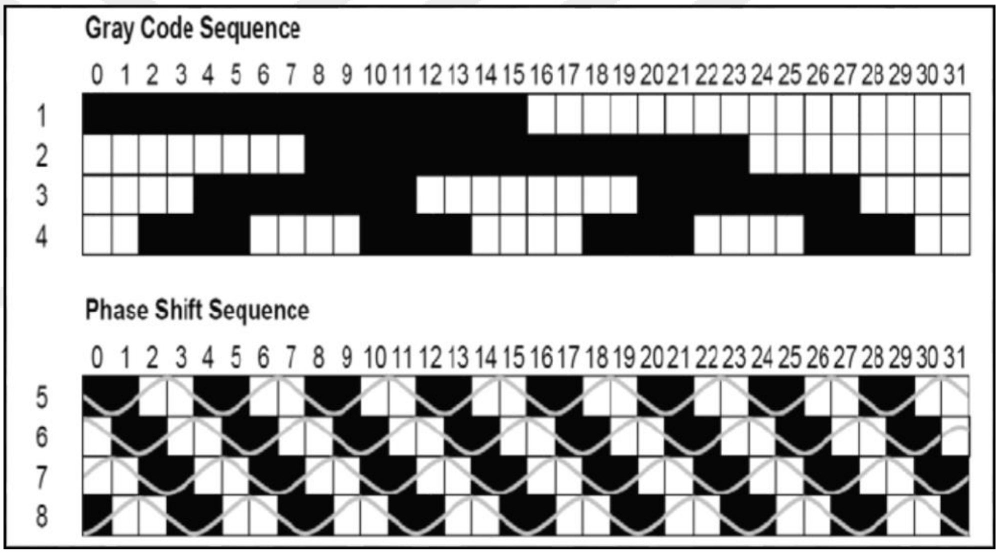

Source: Structured-Light 3D Surface Imaging: A Tutorial, By Jason Geng, 2011.

2.1.5 Photometric

Woodham founded the Photometric stereo (Woodham, 1989), is an irregular tactic to form from masking. It approximates local external surface positioning by using a series of imageries of the same surface occupied from a similar standpoint, but beneath lighting of different angles (Basri & Jacobs, 2006) as shown in figure 2.7. Therefore, it resolves the ill-posed issues in a figure from shading by using several images. This tactic demands the entire sources of light to be direct light and it approximates only the local surface location. It assumes connections of the 3D surface and requires an initial point, meaning a point on the surface of the object (x, y, z) coordinates must be identified for its 3D re-establishment processes.

Figure 2.7: Photometric Stereo Scheme.

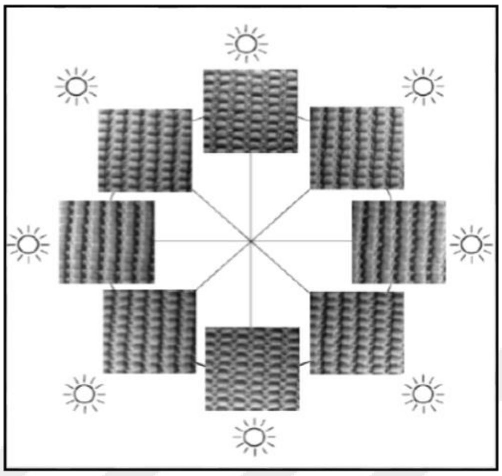

Source: Structured-Light 3D Surface Imaging: A Tutorial, by Jason Geng, 2011.

2.2 FULL-FRAME SPATIALLY VARYING COLOR PATTERN (SINGLE SHOT)

Being unable to acquire a 3D image from a dynamic object is considered as the most major disadvantage of the sequential projection techniques, but for the Full-frame color pattern method we can rid of this issue. We can present few single-shot projection techniques which takes advantage of the information on colors and unique encoding scheme in the projected patterns which requires capturing only one image of the 3D object under the illumination of the colored patterns.

2.2.1 Rainbow 3D Camera

We can illustrate the basic concept of this technique in figure 2.8. Dissimilar from the traditional stereo, which needs to abstract consistent structures from a couple of stereo images to compute the distance rate. The Rainbow 3D (Geng, Structured-light 3D surface imaging:, 2011) camera schemes on the object surface a spatial variable wavelength enlightenment.

The projector's stationary geometry creates a one-on-one resemblance between a particular spectral wavelength λ, and the projection angle, Θ, of a plane of light, accordingly, the landmarks on all object surface points can be easily identified.

With an identified standard (baseline) B and an identified inspecting angle,

As the standard baseline B is identified as well as the angel α, by using a frank triangulation principle, we can calculate the 3D distance values identical to each separate pixel. Then, the full framed 3D image could be obtained with one single snapshot with a frame rate of the camera (30 frames/s or higher).

Figure 2.8: Rainbow 3D Camera.

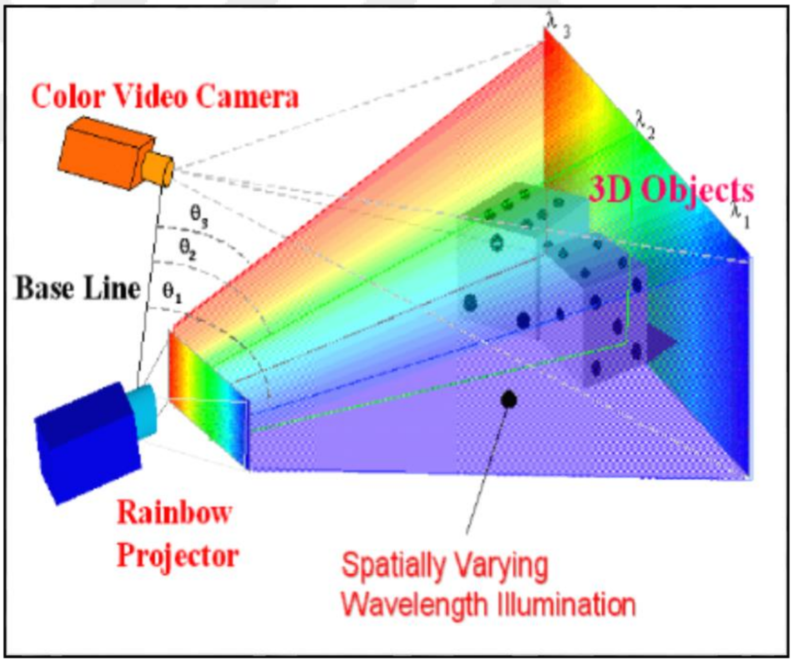

Source: Structured-Light 3D Surface Imaging: A Tutorial, By Jason Geng, 2011.

2.2.2 Infinitely Capricious Color Coding

We can combine numerous endlessly wavering color patterns to encrypt a spatial position info (Heike, Upson, Stuhaug, & Weinberg, 2010). For instance, we can build a concentration variant pattern for every color channel, when we combine those color waves, patterns in separate color channels shapes an unceasingly changing color pattern. Figure 2.9 is a sample of concentration variant patterns for three preservative channels of primary colors. As they are combined, it will shape a rainbow color image. We should note that this pattern of color does not essentially track an undeviating variant connection in color range. The decoding outline can be easily concluded and implemented, since the relations between the contributions from each color channel are well-known.

Figure 2.9: An Endlessly Wavering Color Coding Pattern.

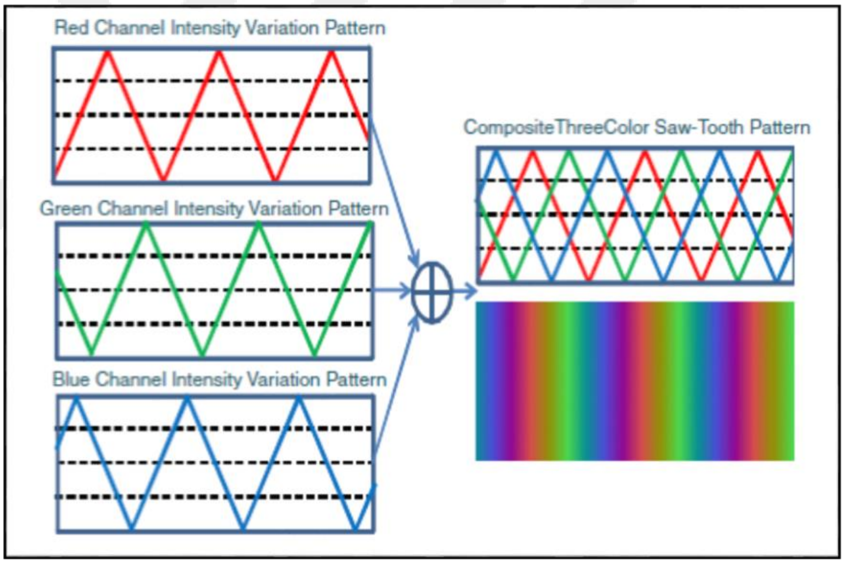

Source: Structured-Light 3D Surface Imaging: A Tutorial, By Jason Geng, 2011.

2.3 STRIPE INDEXING

It is essential to use Stripe indexing to accomplish solid 3D surface re-establishment, because sometimes the projected patterns are observed in a different order from the source. This issue caused by the parallax of characteristic remaining on 3D surface imaging systems based on triangulation and the chance to lose patterns from the captured image cause of the obstruction of the scanned object 3D surface geographies. We can present couple exemplary stripe indexing methods.

Figure 2.10: Stripe Indexing Using Colors.

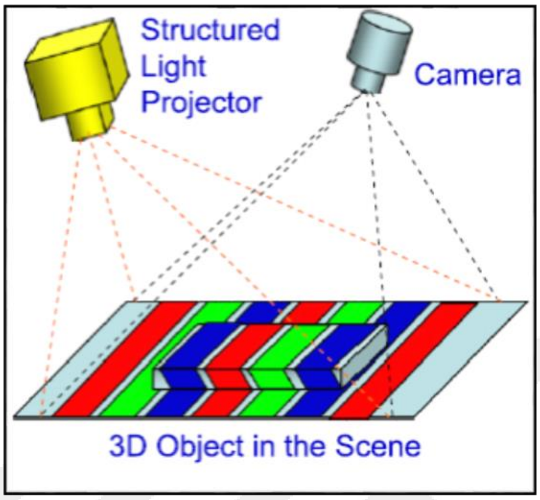

Source: Structured-Light 3D Surface Imaging: A Tutorial, By Jason Geng, 2011.

2.3.1 Stripe Indexing Using Colors

Sensors of Colored images regularly have dependent three obtaining channels, every one of them matching a continuous strip. If we need to create an endless number of colors we can combine the values of these three color components linearly, for example, three channels of 8-bit can give us 2^{24} colors each are different from the other. This can result in an enhanced and an accurate 3D image scanning with a reduced acquisition time. In figure 2.10, the opacity issue faced by phase-shift or multi-stripe methods can be modified by using the color of stripe indexing in projecting patterns with monochromic stripes (Boyer & Kak, 1987). This sort of structure can accomplish real-time 3D surface scanning ability. Also, it is probable to code several arrays into one single color projected image, as every pattern having an exclusive color. For decreasing the decoding inaccuracy ratio, we can select a combination of colors which in this combination every color will have a maximum space from the other colors. We know that the greatest number of colors in the combination is restricted to the space between colors that produce less cross talk in the attained images.

2.3.2 Stripe Indexing Using Segment Pattern

To differentiate single band from other bands we can use distinctive segment patterns to every projected stripe as shown in figure 2.11 (Maruyama & Abe, 1993). Therefore, when executing 3D re-establishment, this procedure can use the exclusive fragment patterns of each band to differentiate them. This technique of indexing, is fascinating and crafty, but it merely applies to a three dimensional object with a surface which is even and constant if the pattern alternates cause of the surface form is not harsh. Or else, it can be very challenging to recuperate the exclusive section pattern, because of the distortion of the stripes and/or incoherence of the targeted object surface.

Figure 2.11: Illustration of Segment Pattern with Stripe Indexing.

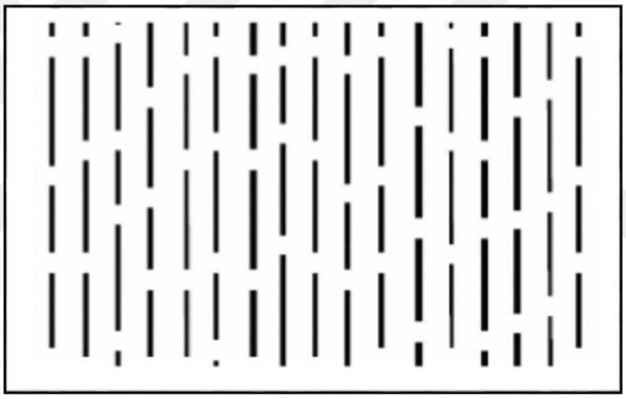

Source: Structured-Light 3D Surface Imaging: A Tutorial, By Jason Geng, 2011.

2.3.3 Using Repeated Gray-Scale Patterns in Stripe Indexing

It is probable to organize the concentration stages of stripes, such that any set of stripes if more than two intensity levels are used (a skimming window of N stripes) as it has a special concentration pattern within a duration of the distance (G. Durdle, J. Thayyoor, & J. Raso, 1998). For instance, if three (black, gray and white) gray-levels are used we can design a pattern as shown in figure 2.12. The pattern matching process begins with corresponding of assimilated image concentration with projected concentration pattern.

A further examination is executed on the sub-gray level sequence match once the match is located, for instance, three-letter series GWB, WGB, etc.

Figure 2.12: Stripe Indexing Using Repeated Gray-Scale Pattern.

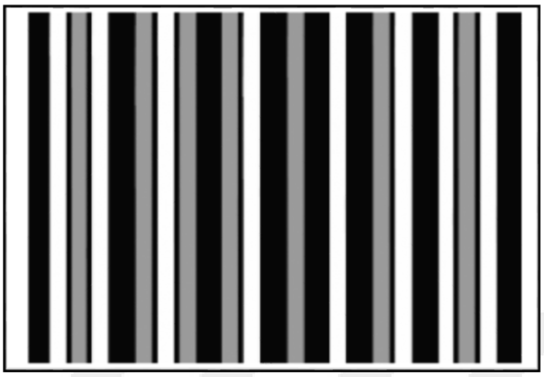

2.3.4 Using De Bruijn Sequence in Stripe Indexing

The De Brujin (MacWilliams & Sloane, 1976) is a cyclic word which n represents sequence rank and K is size of alphabet as each K^n Words appear only once every time we travel the circle (either clockwise or counterclockwise). If we assume n = 3 and k = 2 the alphabet will be (0, 1) as shown in figure 2.13. We will come across each of the three digit patterns as we calculate $K^n = 2^3 = 8$ the sequence will be 000, 001, 010, 011, 100, 101, 110, 111 and we will encounter each one of them only once. Meaning, in De Bruijn sequence, subsequences are not connected in any way to each other, giving De Bruijn a special quality which can be applied in constructing a sequence of stripe pattern with unique pattern variations in each stripe that never repeat themselves (Fredricksen, 1982). Applying this method eases the task of decoding patterns. A De Bruijn graph is the term of the graph related to De Bruijn sequence (Pajdla, 1995)

Figure 2.13: Meek Sample of De Bruijn Sequence.

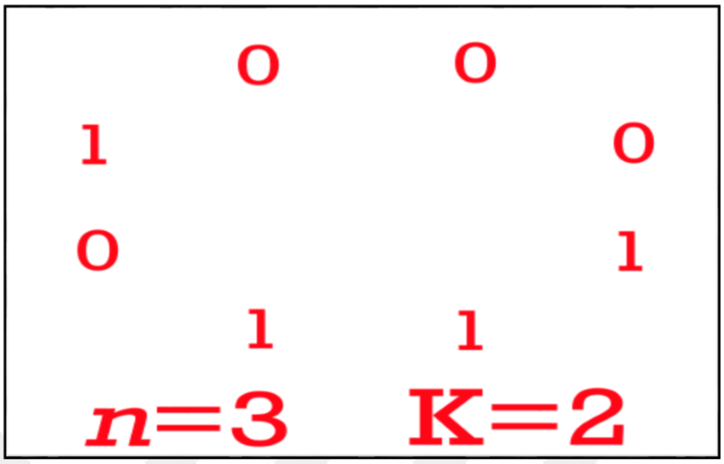

Figure 2.14: Sample of (k=5, n=3) color-indexing based on De Bruijn sequence.

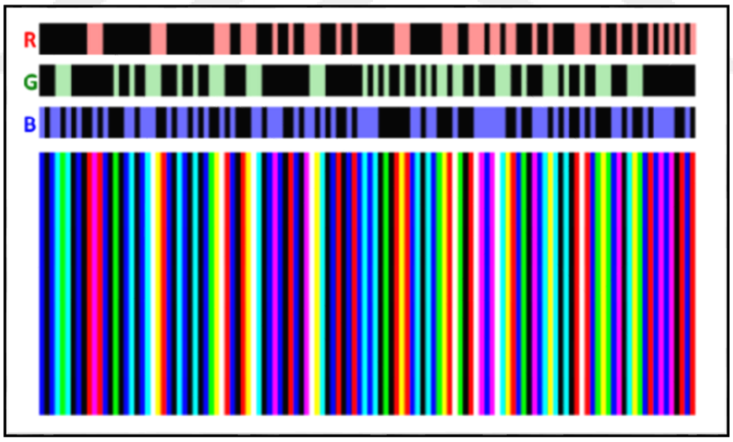

Source: Structured-Light 3D Surface Imaging: A Tutorial, By Jason Geng, 2011.

Applying De Bruijn sequence on a combination of colors (Red, Green, Blue) to create a strip of color-indexed leading to eight numbers of colors (2^3) which is the maximum of the combination of three colors, but this will result seven colors since we don't use (0, 0, 0). By creating a De Bruijn sequence where k = 7 and n = 3 we can solve this problem. But this will result to a sequence number of too many stripes, which is 343, therefore we can reduce De Bruijn set sequence k to 5 and on to 3 (L. Zhang, B. Curless, & M. Seitz,

2002) which will reduce thstripees number to 125. The stripes, which are near to each other must have different colors otherwise it will result to some stripe width being doubled or tripled, which will the 3D algorithms of reconstruction, and this can be applied with ease by using apparent of XOR. This is considered an important constraint in sequence of color-indexing stripes constructions in using De Bruijn method. We show in figure 2.14 results of a set of real stripe pattern of color-indexing. As we can note that all stripes near to each other have different colors in this stripe. In 3D surface imaging applications several implementation variations can be applied in generating unique gray scale indexing, color-indexing, and other kinds of patterns using De Bruijn.

2.4 SPATIAL 2D GRID PATTERNS USING GRID INDEXING

In this method we basically label each sub-window uniquely in the 2D patterns which are projected, this will result to a pattern in the sub-window being identifiable and unique with the consideration of its 2D position.

Figure 2.15: PRBA of A 31 X 33 with Sub-Window Size 5 X 2 and Primitive Polynomial of Amount 10.

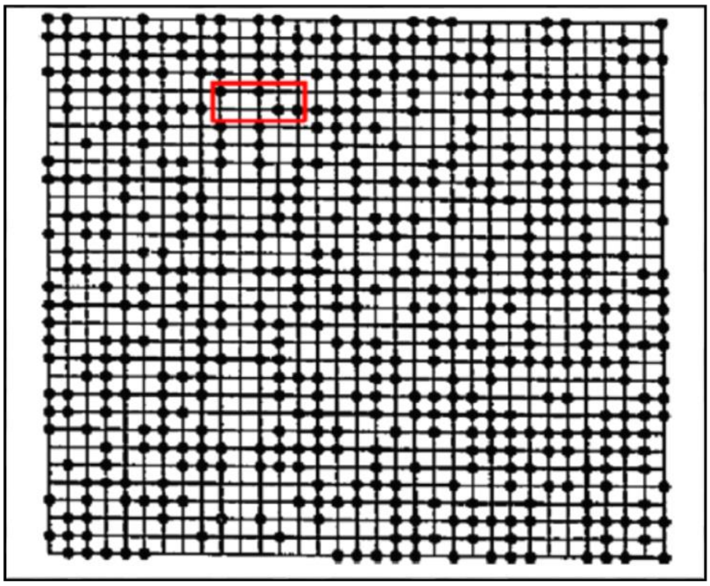

Source: Structured-Light 3D Surface Imaging: A Tutorial, By Jason Geng, 2011.

2.4.1 (PRBA)

(PRBA) stands for Pseudo-random binary array. It is one of the Grid-indexing technique that can create locations of grid which by dots and other patterns can be marked, producing in each sub-window a coded pattern that is unique. Using a sequence of pseudo-random, PRBA is represented by an encoded array of n1 x n2, thus, every sub-window is matchless which k1 by k2 sliding over the entire array and it describes the absolute coordinates within the array (I, j). Using the primitive polynomial modulo 2^n a technique we can produce binary array's coding pattern according to pseudo-random binary sequence (Moigne & Waxman, 1985). As 2^n- 1= $2^{k1\,k2}$ – 1, n1 = 2^{k1} – 1, n2 = 2^n – 1/ n1. Figure 2.15 illustrates a sample of a PRBA, where k1 = 5, k2 = 2, therefore n1 = 31, n2 = 33.

2.4.2 Using Mini-patterns as Code Words

We can use multivalued (PRA) pseudo-random binary array instead of using a (PRBA) Pseudo-random binary array. Using mini-pattern in representing every value as special code word which will create a projectable pattern with grid-indexed (Griffin, Narasimhan, & Yee, 1992). Converting pseudo-random array (PRA) with multiple value into patters for projection with distinct sub-windows by using code words which are specially defined, as shown in figure 2.16 a PRA with three values and a set of code words with mini-patterns.

Figure 2.16: Grid Indexing, Code Words By Using Mini-Patterns.

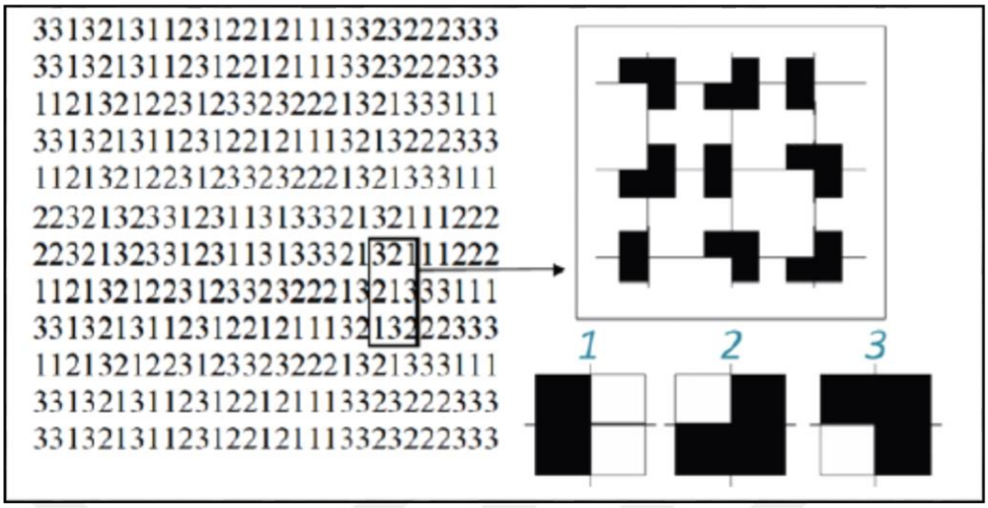

Source: Structured-Light 3D Surface Imaging: A Tutorial, By Jason Geng, 2011.

2.4.3 Color-Coded Grids

To achieve the 2D grid indexing, we can use another strategy, by using color codes for horizontal and vertical stripes (Desjardins & Payeur, 2007). Depending on applications, the vertical and horizontal stripes coding structures can both be the same or completely altered as shown in figure 2.17. It gives no assurance of the individuality of sub-windows, but informing the communication of the stripes, which are colored in both ways can aid the decoding in utmost circumstances. The shrill lines of the grid might not be as dependable in pattern abstraction as the other patterns (squares, dots, etc.).

Figure 2.17: A Sample of Color-Coded Grids.

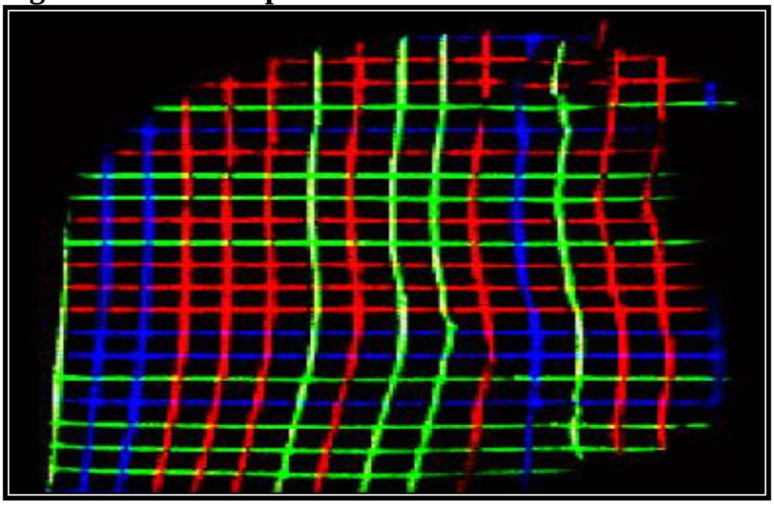

Source: Structured-Light 3D Surface Imaging: A Tutorial, By Jason Geng, 2011.

2.4.4 2D Color-Coded Dots Arrays

We can also use other methods to generate a PRA. One is comparatively instinctive to apply in algorithms of compute (Desjardins & Payeur, 2007). In figure 2.18 for example, shows array of 6 x 6 with size of sub-window 3 x 3 using (Red, Green, Blue) as coded words. This method was represented to create an array that reserves the sub-windows' distinctiveness, but probably not all possible sub-window patterns will be exhausted. The procedure of computing is to first fill with random chosen pattern the top left corner of the 6 x 6 array, and then adding a random code word to the three-element column at the right. And before adding a column of such, the uniqueness are verified of the sub-window. Thus, until all columns are filled and a sub-window distinctiveness is verified, we keep adding the columns with random code words. Doing the same by adding random rows in bottom direction from the position of sub-window. Then, along the diametrical direction, we add other random code words. Thus, this procedure should be repeated until we fill with colors all the dots. This method has achieved good results in many cases, but in some computing procedure the PRA not all code words and array sizes are generated, so this method does not guarantee positive results. In figure 2.18, a 20 x 18 dimensional pseudo-random array is represented as an example.

Figure 2.18: Color-Coded Dots with 2D Array.

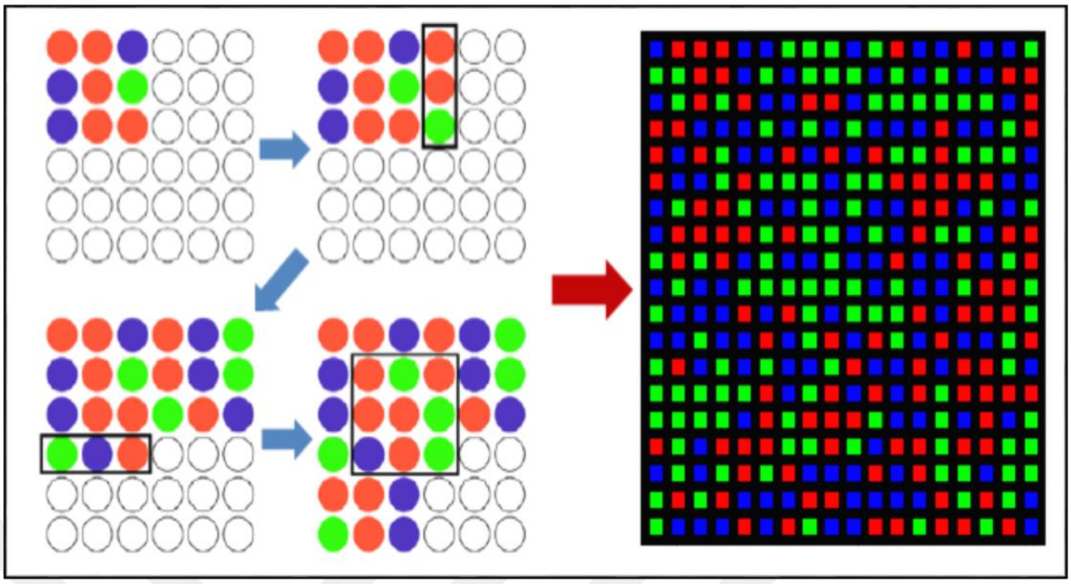

Source: Structured-Light 3D Surface Imaging: A Tutorial, By Jason Geng, 2011.

2.4.5 Hybridized methods

We know there are many prospects to advance particular feature(s) of 3D imaging technologies enactment by merging several encoding structure discussed previously. Figure 2.19 illustrates a sample. As two of one dimensional stripe codes combined into two dimensional grid indexed pattern.

Figure 2.19: Two of One Dimensional Stripe Codes Combined Into Two Dimensional Grid Indexed Pattern.

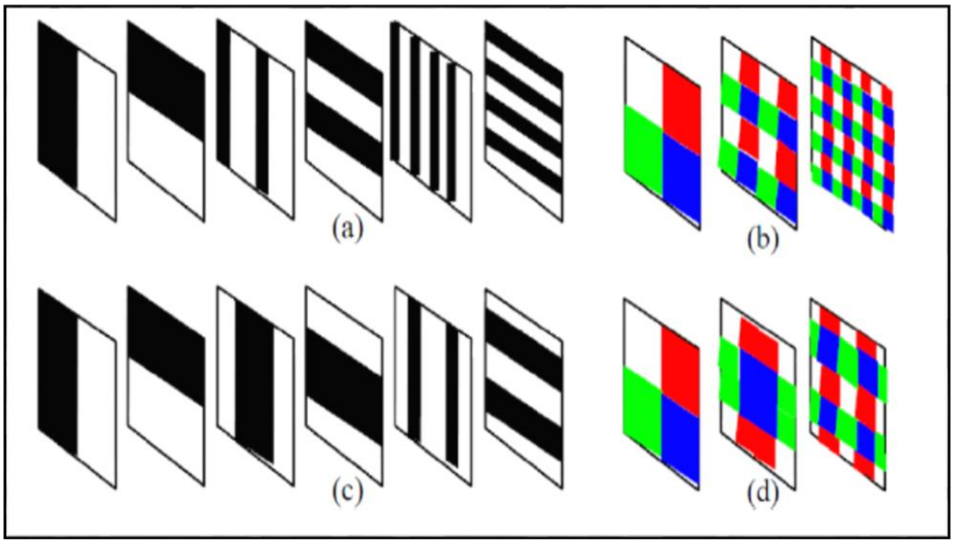

Source: Structured-Light 3D Surface Imaging: A Tutorial, By Jason Geng, 2011.

3. CALIBRATION METHODS

By using special calibration patterns and planes, the geometric misrepresentations caused by optics and viewpoint have to be compensated by calibration (Geng, Advances in Optics and Photonics, 2011). It is important for an efficient and active photogrammetric method to recognize the camera geometry. This can be accomplished by using a planer test field and a convergent structure. And for the sake of the easement the calibration process, we seek more than one calibration stage. The techniques of projector and camera calibrations are one of the most crucial parts of 3D surface imaging technologies. As it plays a perilous role in creating accuracy measurements in 3D imaging systems, as the camera calibration is an issue which is well-known in computer vision technologies, but however, in many articles of applications and 3D imaging technique reviews and researches, this main significant characteristic of 3D imaging systems did not receive plenty consideration and attention.

The most vital measure of the 3D imaging technologies which has a significant part in creating the dimension accurateness for 3D imaging technique is the camera and projector calibration, which is distinguished difficulty for computer vision.
One of the common calibration methods is using a planar object black and white patterns as shown in figure 3.1 as it is easy to create and we can print it by a regular printer. Also it has individual angles which can be easily perceived. We start by moving the camera around the planar test field and capture pictures from different angles and distances established on a predefined scheme for the camera settings. As many 3D imaging techniques use 2D optical sensors, the camera calibration techniques, forms a bond among a pixel of a 2D image with a stripe in 3D space where the object point is found. Once defining basic strictures of each camera. They are attached on a steady aluminum contour with a secure convergent arrangement whereas multi-media video projector has previously been secured among them. To define virtual location constraints concerning two cameras the planar checkerboard is used. As both cameras capture a picture. Angles points on checkerboard which now have an exact 3D coordinate from the package modification in earlier stage are used as 3D control points in order to decide six external alignment parameters of all of the two cameras based on collinearity equations.

Camera calibration processes are mainly establishing a connection between a straight line in coordinates of the real world at the location of the targeted object (taking in consideration the lens distortion) and a pixel in 2 dimensional image as coordinates of the optical sensor as most 3D imaging systems use optical sensors 2 dimensional. We can simply characterize the relationships by using a set of substantial standards and an optical sensor as many toolboxes are obtainable which accompany this task [47–49]. In order to achieve a successful camera calibration, it is obligatory to capture several images from different angles for the targeted object.

Figure 3.1: The Planar Target for Calibration.

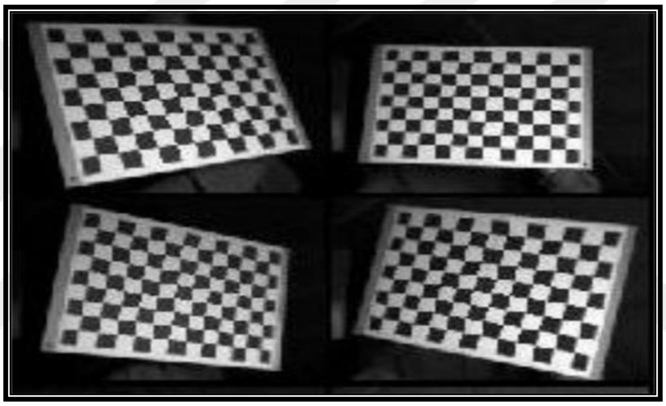

Source: Structured-Light 3D Surface Imaging: A Tutorial,
By Jason Geng, 2011.

3.1 CAMERA CALIBRATION

Considering the real world coordinates of the value of calibration panel planar is Z = 0, we will have every point on the board of calibration $M = [X, Y, 0, 1]^T$ consequently, a holographic matrix connects an object point M and its point on image m:

$$m \sim K[r_1, r_2, r_3, -R_t] \quad [X, Y, 0,1]^T, \qquad \textbf{(3.1)}$$

$$m \sim H[X, Y, 1]^T, \qquad \textbf{(3.2)}$$

As $H = [h1, h2, h3] = K [r1, r2, - Rt]$ is a 3 x 3 matrix demarcated up to a measure, and $r1, r2, r3$ are 3 x 1 column directions of the spin matrix. Seeing that for a matrix of rotation R the direction of column $r1, r2, r3$ is orthonormal, therefore we get:

$$h_1^T (KK^T)^{-1} h_1^T = 0, \quad \textbf{(3.3)}$$

$$h_1^T (KK^T)^{-1} h_1^T = h_2^T (KK^T)^{-1} h_2^T, \quad \textbf{(3.4)}$$

Every holography can give two restrains on the inherent strictures. As $K^{-T}\ K^{-1}$ in the previous calculation is a regularity matrix, we can define it with a 6D vector:

$$A - K^{-T} K^{-1} = \begin{bmatrix} A_1 & A_2 & A_4 \\ A_2 & A_3 & A_5 \\ A_4 & A_5 & A_6 \end{bmatrix}, \quad \textbf{(3.5)}$$

$$a = [A_1, A_2, A_3, A_4, A_{5,} A_6]. \quad \textbf{(3.6)}$$

Knowing that *i*th column route of *H* can be *hi* = [*hi1*, *hi2*, *hi3*]. So we will get;

$$h_i^T A h_j = v_{ij} a, \quad \textbf{(3.6)}$$

Where in in vij = $[hi1hj1, hi1hj2 + hi2hj1, hi2hj2, hi3hj1 + hi1hj3, hi3hj2 + hi2hj3, hi3hj3]^T$. As the two limitations afterwards could be rephrased as an equation of homogeneous. To resolve a, we need minimum 3 images from dissimilar angels or viewpoints. Usually, additional images are used to decrease the consequence of distortion, and a minimum error solution of squares is acquired with remarkable value decay. Lastly, by retreating the energy function below, the outcome can be improved to diminish the re-projection error:

$$\sum_{i=1}^{n} \sum_{j=1}^{m} \left\| m_{ij} - (K, R, t, M_j) \right\|^2. \quad \textbf{(3.7)}$$

3.2 PROJECTOR CALIBRATION

There are two main factors of projector calibration, since the projector considered as a light source, we need to calibrate the intensity to gain evenness of its intensity of illumination. Plus, we have to calibrate it geometrically as a usual camera since it is considered as a reverse camera.

3.2.1 Projector Intensity Calibration

The projector vendors usually change the transformation of gamma with the curve of concentration to increase the contrast. Therefore, while we use the projector as a light source in 3D imaging system we must calibrate it to regain the evenness of the concentration of its illumination. In order to do that, we can project several patterns as test and obtain by optical sensors the patterns which are projected.

We rectify the patterns before being projected in the process of 3D imaging after calculating the inverse function when the connection between the real intensity of patterns which are projected and pixel value of the image is established. This procedure is illustrated in figure 3.3.

3.2.2 Symmetrical Calibration of Projector

The only difference between optical camera sensor and projector optic model is the projection direction, otherwise there is no difference between them, and therefore the projector is considered as a reverse camera. The problem of connecting a straight line in 3D world coordinates and the camera coordinates as pixel in 2D image is caused by revers model.

The key in the calibration of the projector is to know how to establish a correspondence because if we succeed in establishing the correspondence we can easily apply algorithms of camera calibration to calibrate the projector.

Figure 3.2: Concentration calibration of the projector. The blue curvature is a scheme of the formfitting function. The green curvature is the converse function. As for the red line, 3it should be straight as it is corrected intensity.

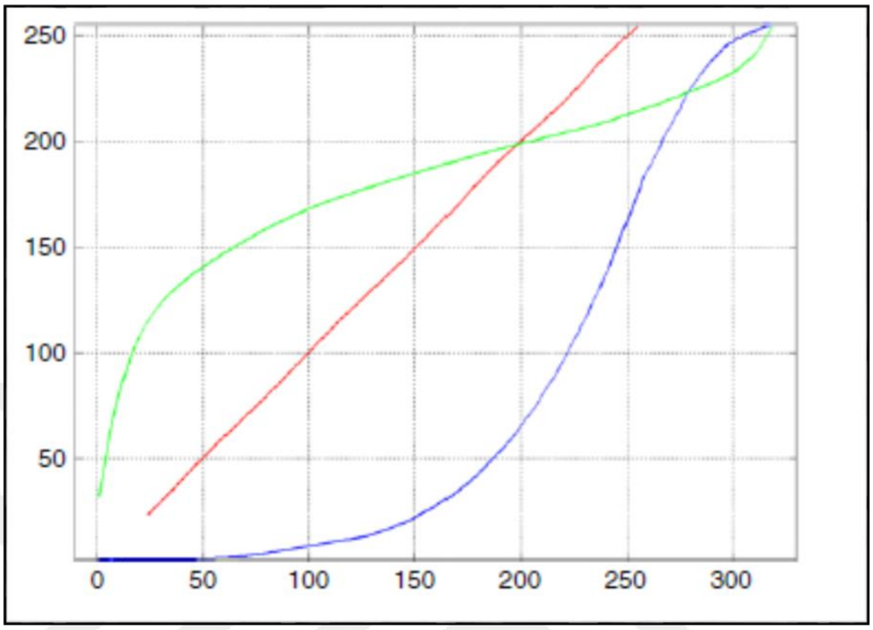

Source: Structured-Light 3D Surface Imaging: A Tutorial,
By Jason Geng, 2011.

Calibration of projector is achieved by applying a calibration scale and a pre-calibrated camera. Firstly, we improve the level of calibration in the coordinates of optical sensor system.

Afterwards, we project the pattern of calibration as shown in figure 3.2 and obtain it by the optical sensor. As the three-dimensional connection between the planer plate and the optical sensor is already established, we can determine the 3D coordinates of the chessboard pattern corner points placed on the plane of the calibration by repeating the projection of the points of the corners on the obtained image which is on the plate of the planer. Lastly, we can calibrate the projector by the assimilated correspondences of points. The accuracy of the calibration in these techniques severely determined by the precision of the optical sensor calibration.

Figure 3.3: Calibration of Dot Array Pattern Used In Projector Calibration.

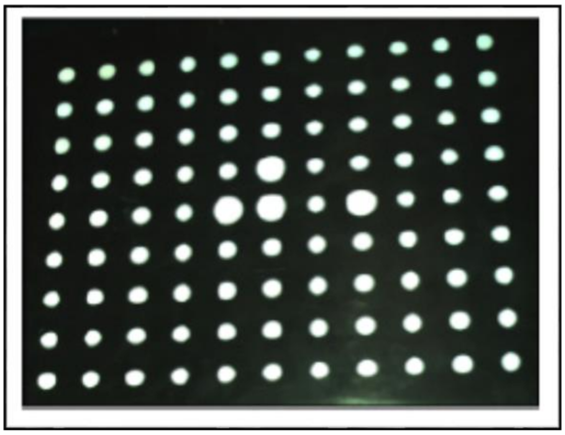

Source: Structured-Light 3D Surface Imaging: A Tutorial, By Jason Geng, 2011.

4. 3D SURFACE IMAGING TECHNOLOGIES PERFORMANCE EVALUATION

Many aspects exists that illustrates a 3D surface imaging system's technical performance. There are three characteristics which are regularly applied as indexes of performance takes place in assessing the 3D imaging technologies according to application's standpoint.

4.1 PRECISION

Quite frequently, because of the innate properties of the design of 3D imaging systems, they may have different accuracies in different directions of (x, y, z). The Accuracy of measurement indicates the maximum perversion of the actual dimension of the 3D object and the measurement value captured by 3D imaging system. Although when it comes to accuracy, manufacturers use different ways with different point of views to characterize its measurements as some might use ± error or improbability, RMS, average error and other standards of statistics.
Thus, we must compare systems in the same framework after understanding the precise significance of any entitlements of performance.

4.2 RESOLUTION

As known in many literatures of optical resolution, it is defined as the capability of a system in an image to clearly distinguish separate lines or points. Same for 3D imaging resolution, it designates the minimum share of the targeted object surface that can be resolved by a 3D imaging technology. Thus, "image resolution" term in some communities of 3D imaging also designates to the system which can capture in a single frame the maximum number of capacity points. Some 3D sensors, for example, with 640 x 480 pixels could create measurement points of 307,200 for an acquisition of a single-shot. We can convert to each other these image resolution definitions if standoff distance, field of view and other factors are known.

4.3 SPEED

Speed of acquisition is significant for scanning objects which is dynamic as the human body, this issue for single-shot techniques in 3D scanning systems is not significant as sequential methods. As for single-shot techniques, frame rate represents the ability to repeat the acquisition of full-frame in short amount of time. Unlike the sequential methods, in addition to frame rate, the issue that needs to be considered is that the object is dynamic (laser scanner for example) while the acquisition is in performed, this will result the obtained 3D image (full-framed) to be not representing a snapshot of the targeted object at the same location point but it turn into a mixture of dimension points captured in different instance of time. Thus, the resulted 3D shape will be distorted and not exact as the original object shape. There is a difference between computation speed and acquisition speed. Some systems are able to process the obtained imagines to create 3D data in much slower frame rate than acquiring the actual 3D images.

We can compare 3D surface imaging systems by using the previously mentioned three indexes of performance. In figure 4.1 we illustrate the primary space of performance in which 3D surface imaging methods may obtain a place, thus we can compare instinctively multiple 3D surface imaging systems. Putting in mind, the reliability and ratio of price/performance of 3D surface imaging systems are also significant aspects which we must take into consideration. There are almost limitless characteristics of indexes performance additionally to the indexes of the primary performance, which can be used to describe 3D surface imaging precise features. Depth of field for example, is one of the additional performance indexes which refers to the distance between 3D imaging system sensors and the actual object which an accurate full-framed 3D image can be obtained. These indexes eventually will reflect to the indexes of the primary performances which are speed, resolution, and precision. There are also other features that can be used to describe the performance of 3D imaging systems, which are field of view, standoff distance, and the baseline. Standoff distance is usually limited for 3D structured-light imaging systems because of the limited power of the light of the projector, although laser scanning systems can spread to miles of distance. Eventually, we should judge a 3D imaging system by its whole performance in anticipated applications, for all methods and systems have their own pros and cons.

Figure 4.1: Main Performance Space of 3D Surface Imaging Systems.

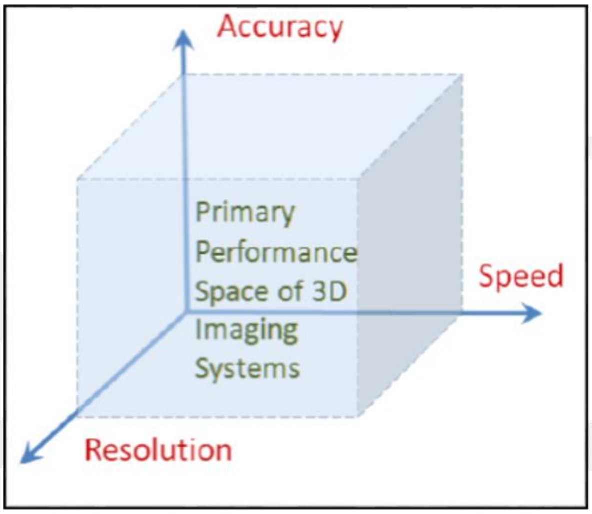

Source: Structured-Light 3D Surface Imaging: A Tutorial, By Jason Geng, 2011.

5. ILLUSTRATIONS OF 3D SURFACE IMAGING APPLICATIONS

There are plenty applications that we will be unable to mention in this paper, but we can provide many interesting application examples which are illustrative and motivating but are not comprehensive.

5.1 3D FACIAL IMAGING

One of the perfect objects for 3D imaging is Human body parts. We know that all human parts are different and there isn't a digital human body parts model (CAD). So, for application purposes, all body parts are needed to be scanned by 3D imaging. In Figure 5.1 illustration of a sample of a facial 3D image captured by a 3D optical camera. Facial 3D images have plenty of applications as facial 3D recognizer and plastic surgeries and 3D face models modified as gifts.

5.2 3D IMAGING OF DENTAL APPLICATIONS

Regularly, if we needed to capture an entire surface of the targeted area in dental arch we need to capture multiple 3D images for that area and to unit these several images with each other. We can use a 3D software which will pierce them flawlessly to create the model of the arch as a whole. Thus if we need to obtain a small section of the dental arch we can use single-shot 3D image. A sample is shown in figure 5.2 of a 3D dental images captured by a 3D camera.

Figure 5.1: Sample of 3D Facial Images Captured By A 3D Camera Created By the Author.

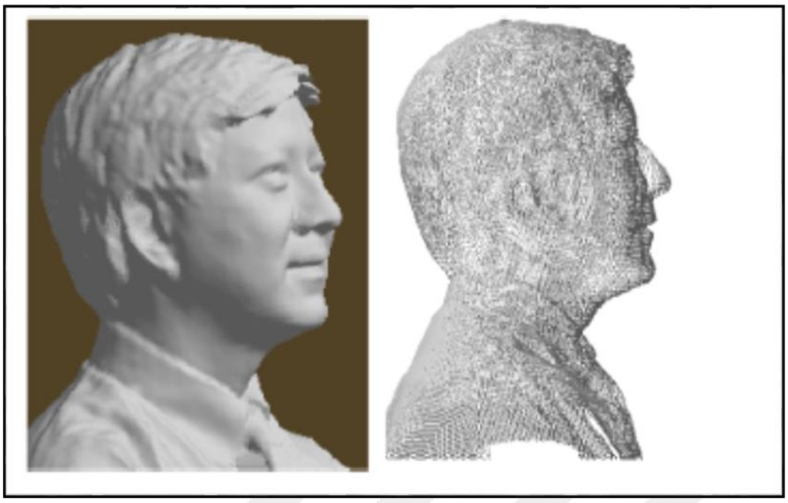

Source: Structured-Light 3D Surface Imaging: A Tutorial, By Jason Geng, 2011.

5.3 PLASTIC SURGERY APPLICATIONS

By the advancement of 3D imaging systems, we are now enabled to process a plastic surgeon to obtain and display the patient's body parts' 3D surface for valuation, pre-surgery therapy preparation, post-treatment confirmation, patient statement, and certification. The 3D images of a body part which are captured for surgery purposes can be used by both doctor and patient to inspect virtual conclusions based on transplant choice, supporting in defining the fitting implant particular volume capacities and probable irregularity.

5.4 EAR IMPRESSION 3D MODEL FOR A HEARING AID CUSTOM-FIT

Unfortunately, 360 million people globally grieve from some hearing damage degrees, based on the statistics from the World Health Organization (WHO). The existing procedure of industrial hearing assistances of custom-fit is proceeding concentrated and aches about one third remake-repair-return ratio.

And now the technology of 3D imaging had almost replaced with the customary physical impression, leading to a method which removed the time and cost related to an error- apt and rough procedure. The digital imprints allow hearing assistance industrialists to gain benefits of the newest advance in computer-aided-design (CAD) and manufacturing (CAM) skills and harvest a custom-right hearing assistance device in a short amount of time frame. In figure 5.3 represents a sample of 3D images of an ear imprint captured by a 3D camera. More vital, the digital imprint technology to be advanced here might increase the superiority of fit, therefore improving the hearing operations for damaged-ears patients.

Figure 5.2: Samples of 3D Dental Images Captured By A 3D Camera.

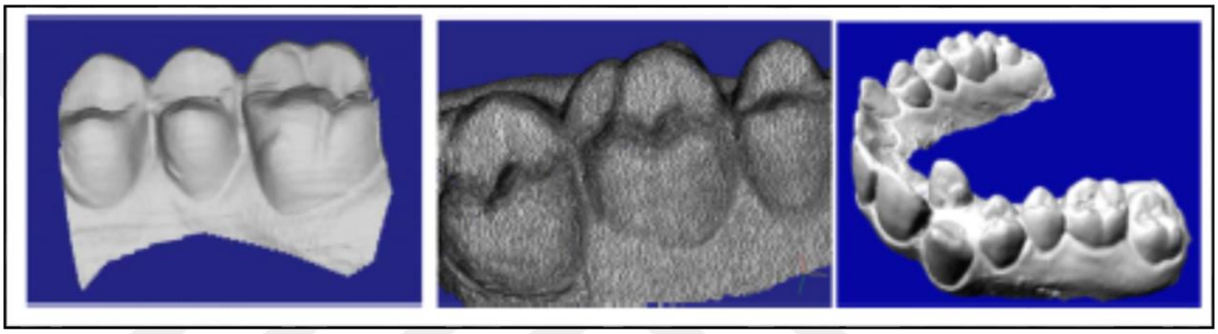

Source: Structured-Light 3D Surface Imaging: A Tutorial, By Jason Geng, 2011.

Figure 5.3: Example of 3D Images of An Ear Imprint Captured By A 3D Camera.

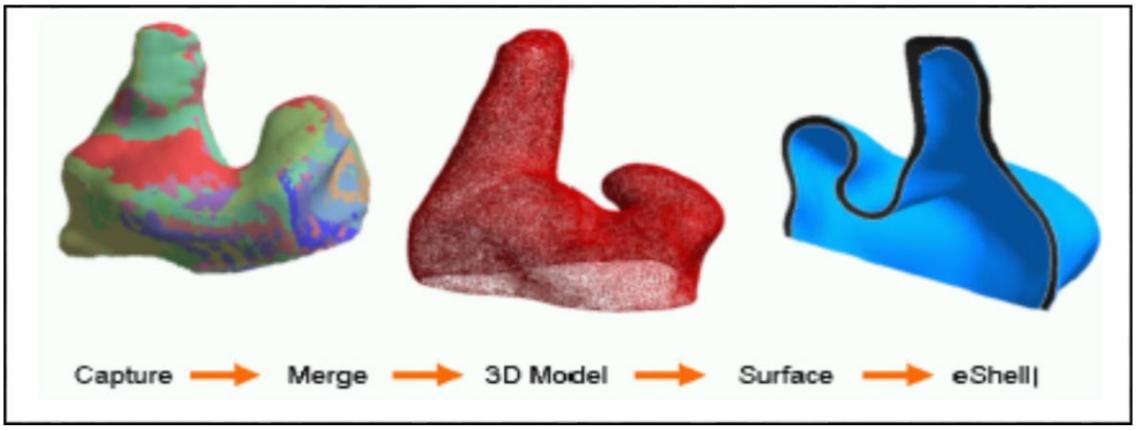

Source: Structured-Light 3D Surface Imaging: A Tutorial, By Jason Geng, 2011.

5.5 REVERSE ENGINEERING USING 3D IMAGING

Designers while designing an ergonomic product they require the physical touch of the product to approach the design with more satisfying way. Therefore, manual procedures are used to observe the shape and optimize it and finalize it until reaching to more favorable design. Then, the prototype is improved by converting it to a 3D CAD file by applying the technology of 3D surface imaging systems. As shown in figure 5.4, a sample CAD file for a mouse designed by the Arthur which is converted to a digital data.

Figure 5.4: Sample of 3D CAD of A Mouse Plan Captured By Using A 3D Imaging System.

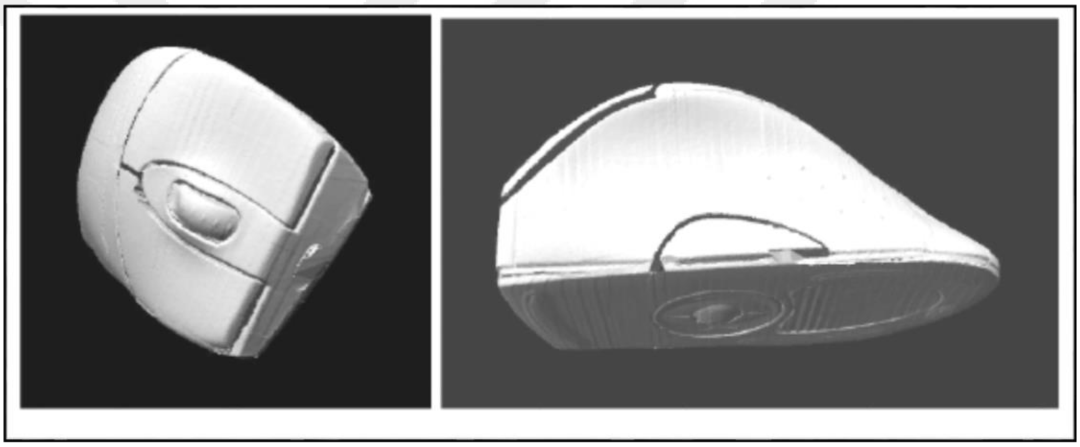

Source: Structured-Light 3D Surface Imaging: A Tutorial, By Jason Geng, 2011.

5.6 3D AIRBAG ANALYSIS USING 3D IMAGING SYSTEM

Many manufacturers use a rapid 3D imaging system to study the performance of air bags giving them the capability to optimize the design for additional safety insurance of the passengers. Thus, the task of capturing the dynamic behavior of the airbags during detonation is extremely tough. But now with 3D sequential imaging technologies this task can be accomplished with accurate and high-speed acquisition. As shown in figure 5.5 the sequential high-speed acquisition was able to capture a series of images during the detonation test of the airbag. The captured data can be used to improve the performance of the critical status of designing airbags in different instants of their rapid explosion stages.

Figure 5.5: 3D Imaging System With High-Speed For Airbag Dynamic Modeling During Expulsion.

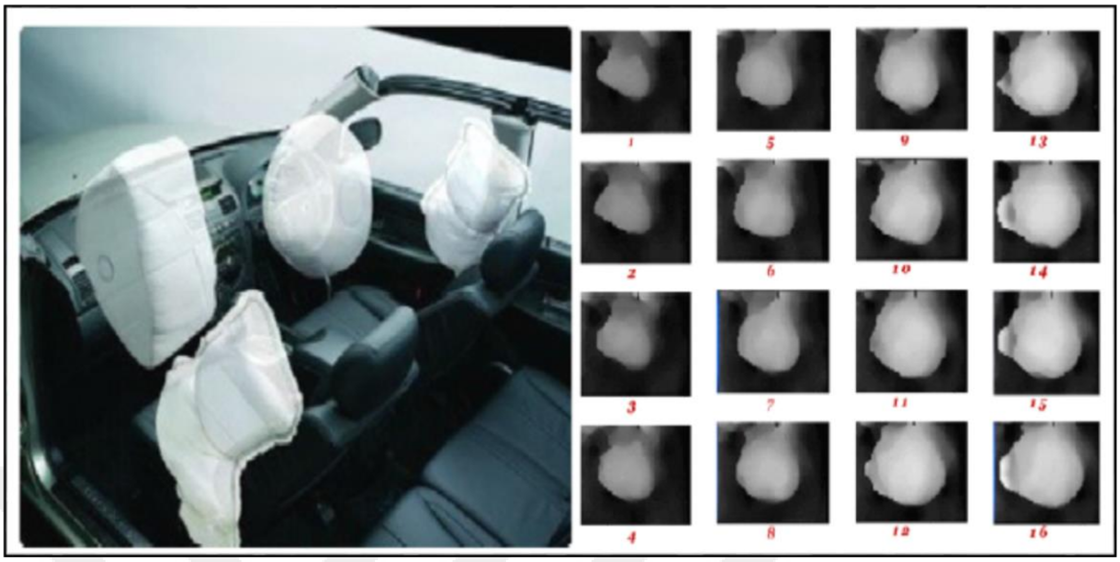

Source: Structured-Light 3D Surface Imaging: A Tutorial, By Jason Geng, 2011.

5.7 DOCUMENTING OBJECTS OF CULTURAL HERITAGE USING 3D IMAGING SYSTEMS

Converting cultural heritages into digital data unlocks many peritonitis and it does not restrict to documenting extremely valuable objects, but also it offers the capacity for the special designers to reconstruct cracked or broken areas, which require a highly accurate 3D model for the object (Akca, Mediterranean Arhaeology and Archaeometry, 2011). 3D imaging technologies make this challenging task much easier with multiple projected pattern images for higher resolution enables the designers to obtain an accurate model for the object. In figure 5.6 designer uses 3D structured-light imaging system to reconstruct the statue of Heracles, which the two body parts were found in different locations. Thanks to 3D imaging technology the operation was successful and the statue now is located in Antalya Museum in Turkey.

Figure 5.6: Using 3D Structured-Light Imaging System to Reconstruct the Weary Heracles Statue.

Source: 3d Modeling of Cultural Heritage Objects with a Structured Light System, 2011.

5.8 ACCIDENT SCENE INVESTIGATION USING 3D IMAGING TECHNOLOGY

Collecting data from an accident scene can cost time and much effort by the investigators and police officers. The Highways agency started a research project in 2006 to create a 3D imaging system which allows to obtain and digitize the whole collision scene within just minutes (Rusted, Accident Investigation Background, 2013). In 2008 the project was successful and currently being used to investigate accident scenes by creating a scene of the collision and reconstructing the accident area with 360 degree detailed environments. Usually this process forces the investigators to block the accident area and stop the flow of the traffic until the manual investigation procedures are over. With 3D imaging system we can use the data to create animations of the accident for analyzing the actual event which then can be used as evidence. Figure 5.7 illustrates accident scenes captured by 3D imaging systems for investigation purposes.

Figure 5.7: Accident Scenes Captured By 3D Imaging Systems for Investigations.

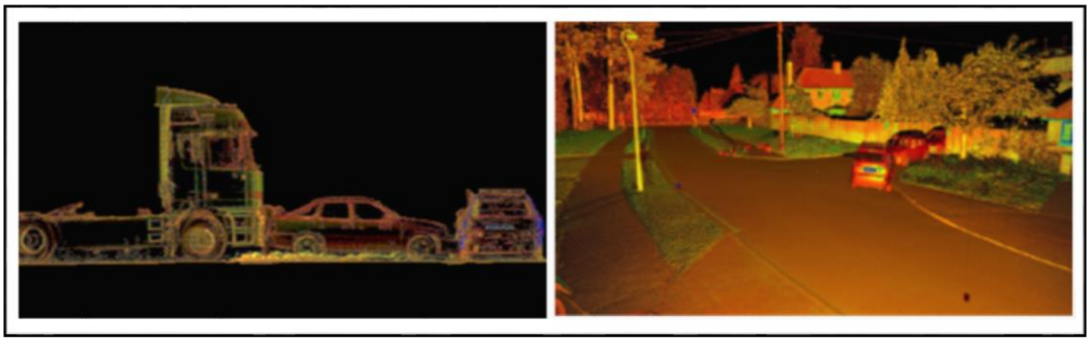

Source: Crash Investigation and Collision Reconstruction, leica-geosystems.us website.

6. THE IMPLEMENTATIONS

Based on the methods are available currently, we will choose two finest techniques and implement them so we are able to study the results and compare the advantages and disadvantages. The most common methods which are used now days are probably the binary coded patters and the gray coded shifting patterns which we will specify their properties in detail.

6.1 USING PHASE-SHIFTING PATTERNS

To choose which technique we should use for our project, we must first take in consideration the pros and cons of each technique. After a time taking decision we realized that the gray-coding levels and phase-shifting patterns are the most reliable techniques and easy to use. Because they rely on binary codes only and they are less sensitive to disfigurations (for example the color of the scanned object and the reflective surfaces). But again, using the binary pattern technique have the disadvantage of their patterns to be blurred as the object moves away from the projector light which can cause major problems in the resulted 3D image. To fix this we used Phase Shifting Patterns as they are pre-blurred and does not be affected by the distance of the object as much as the binary pattern method. The patterns Consisting of: $\cos(\theta - 2\pi/3)$, $\cos(\theta)$, $\cos(\theta + 2\pi/3)$ we get a Phase-shifting scanning patterns as shown in figure 6.1. i1, i2, i3 are the intensities of the projected patterns and the θ is the x or y position in the image.

Figure 0.1: The Intensity of Phase-Shifting Patterns Waves.

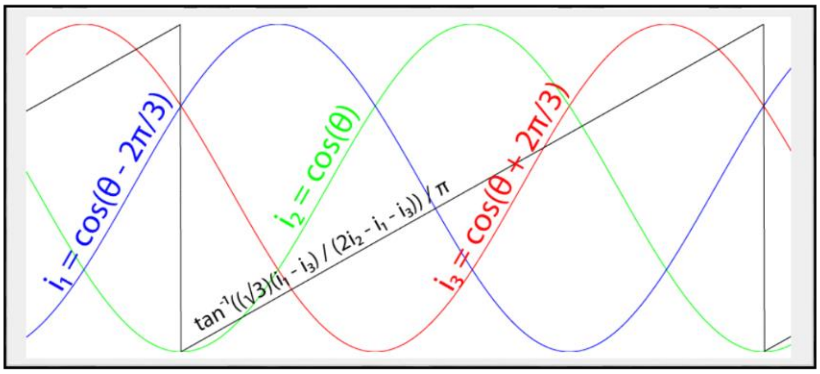

Source: Structured Light 3D Scanning, http://www.instructables.com .

Using Processing application for coding, we managed to create a structured-light 3D imaging system that projects three phase-shifting patterns as we represented in figure 6.2, and we converted each pixel point on the image to a point in a 3D world. Using one camera (Cannon EOS) and a projector (Panasonic PT-LC56E). We captured three pictures and reconstructed them in each session, the results are shown in figure 6.3.

Figure 0.2: The Phase-Shifting Patters Used In Implementing A 3D Surface Imaging System.

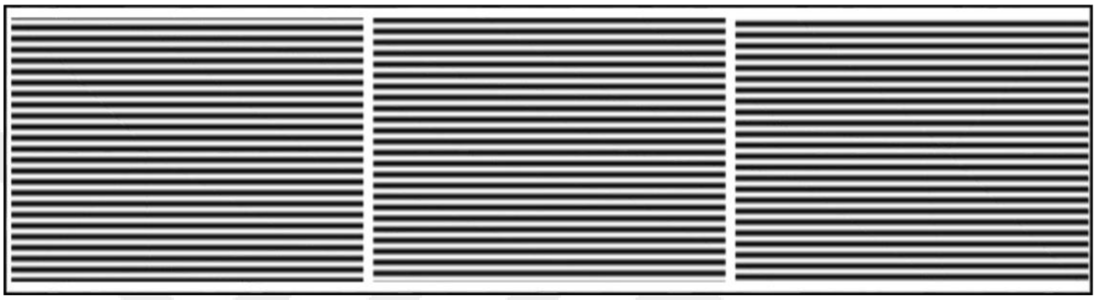

Figure 0.3: The Resulted 3D Images Captured By Using Phase Shifting Technique.

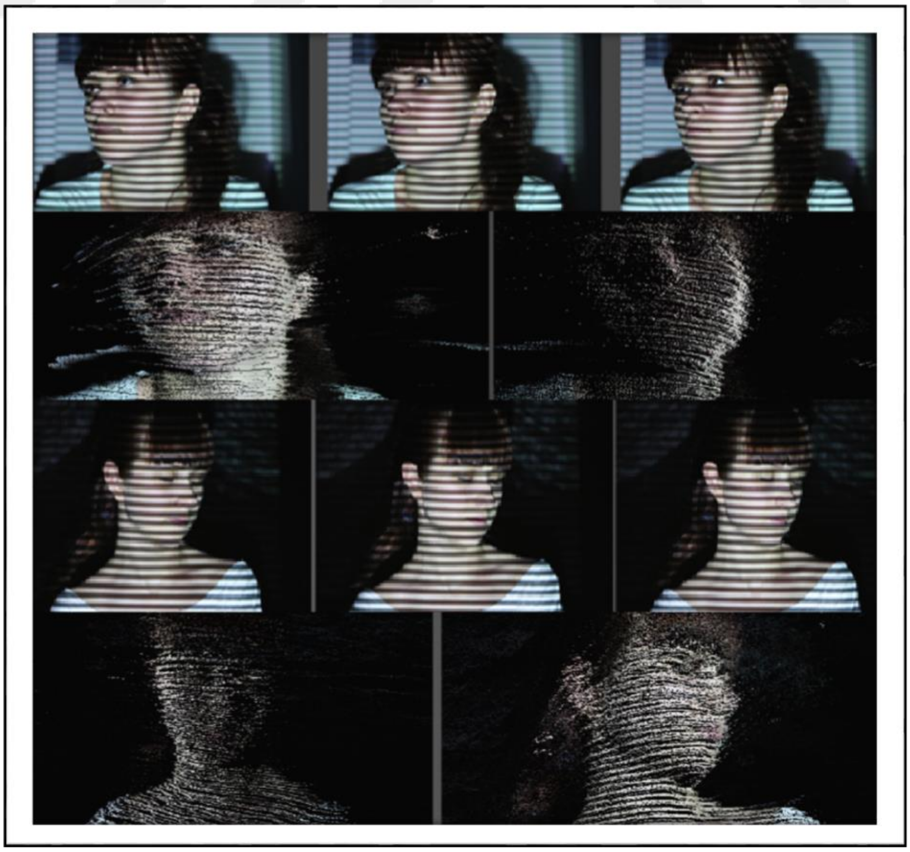

This method is also called Triangulation technique which is based on basic trigonometric principle which takes three values of a triangle and use them to recover the remaining values.

6.2 USING BINARY CODED PATTERNS

In 1981 this method was first anticipated by Altschuler and Posdamer. The static subject is illuminated with multiple set of black and white patterns (horizontal or vertical patterns) as shown in figure 6.4. Currently it is considered as the simplest and most popular method, for it is reliable and easy to implement and use. As we mentioned previously the major disadvantage of this technique is the long period of time spent for the projection of the sequential patterns. But it prevails in the precision of the resulted 3D image. To implement this technique we used Matlab for coding language and Matlab accusation toolbox. We created 41 binary patterns (both horizontal and vertical strips for experimental reasons) which starts from zero as a binary number (black pattern) and a second pattern is resembles 1 as binary number. Using the same projector and camera as we used in phase-shifting patterns and the result had indubitably better quality. As a start, we set the projector on the table and illuminated a calibration board with patterns as shown in figure 6.4 and the camera slightly above the projector to capture the required image from the best angle (the same set up we used for implementing phase-shifting technique). Afterwards we started the calibration by projecting sequence of patterns. We used pinhole camera model for the calibration, this method is well-known. It uses the optical center of the camera and corresponds it to (x, y, z) coordinates in real world projection. The planer consists of black dots and 6 rings 3 in each side of the planer as represented in figure 6.6. As the calibration is done, we used a plastic surfaces as a subjects. We chose a less reflective plastic surfaces to prevent the light being reflected to the optical camera which leads to reconstruction errors and the 3D model would be distorted. The results, indubitably had better quality than phase-shifting method, but certainly it doesn’t mean it overcomes the advantages of using phase-shifting technique. We captured snapshots of the 3D models as shown in figure 6.7 in the process of scanning and the outcome result.

Figure 0.4: Binary Coded Patterns Used In Our Implementation.

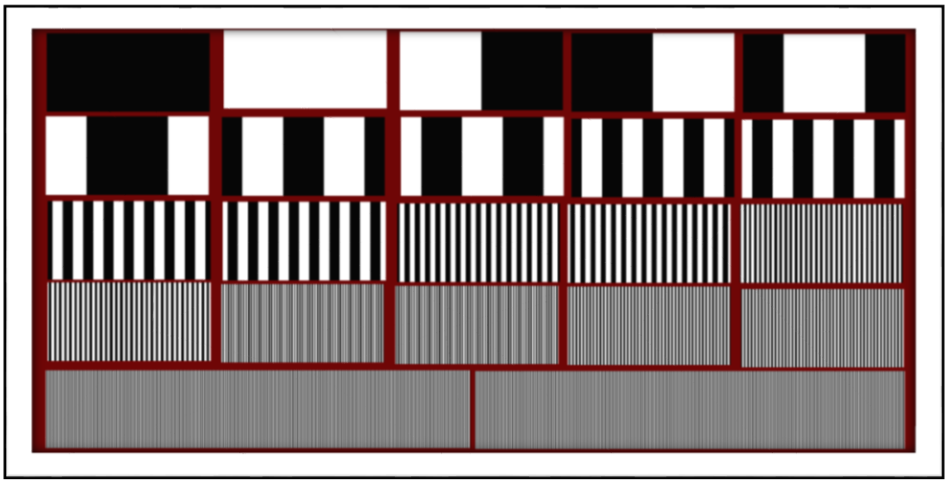

Figure 0.5: Set Up Of The Implementation.

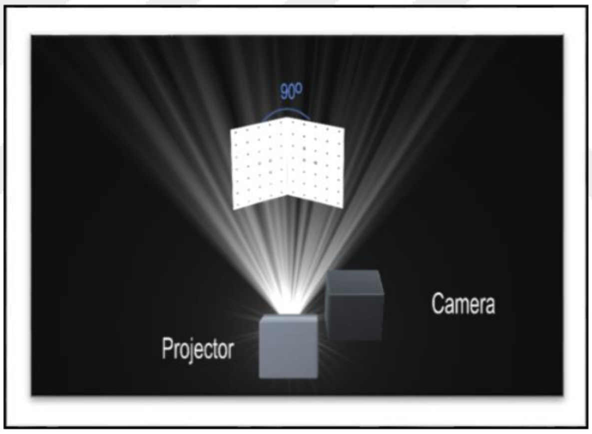

Figure 0.6: Calibration Board.

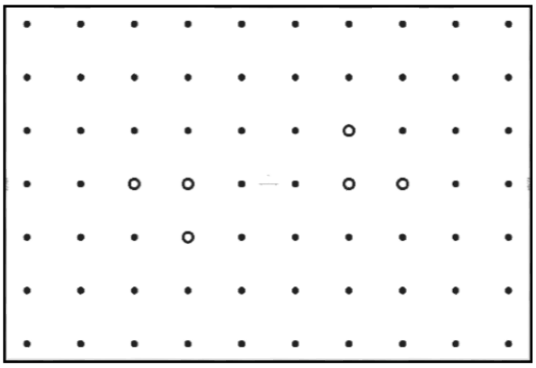

Figure 0.7: Plastic objects Illuminated by Binary Patterns and Captured its 3D Model.

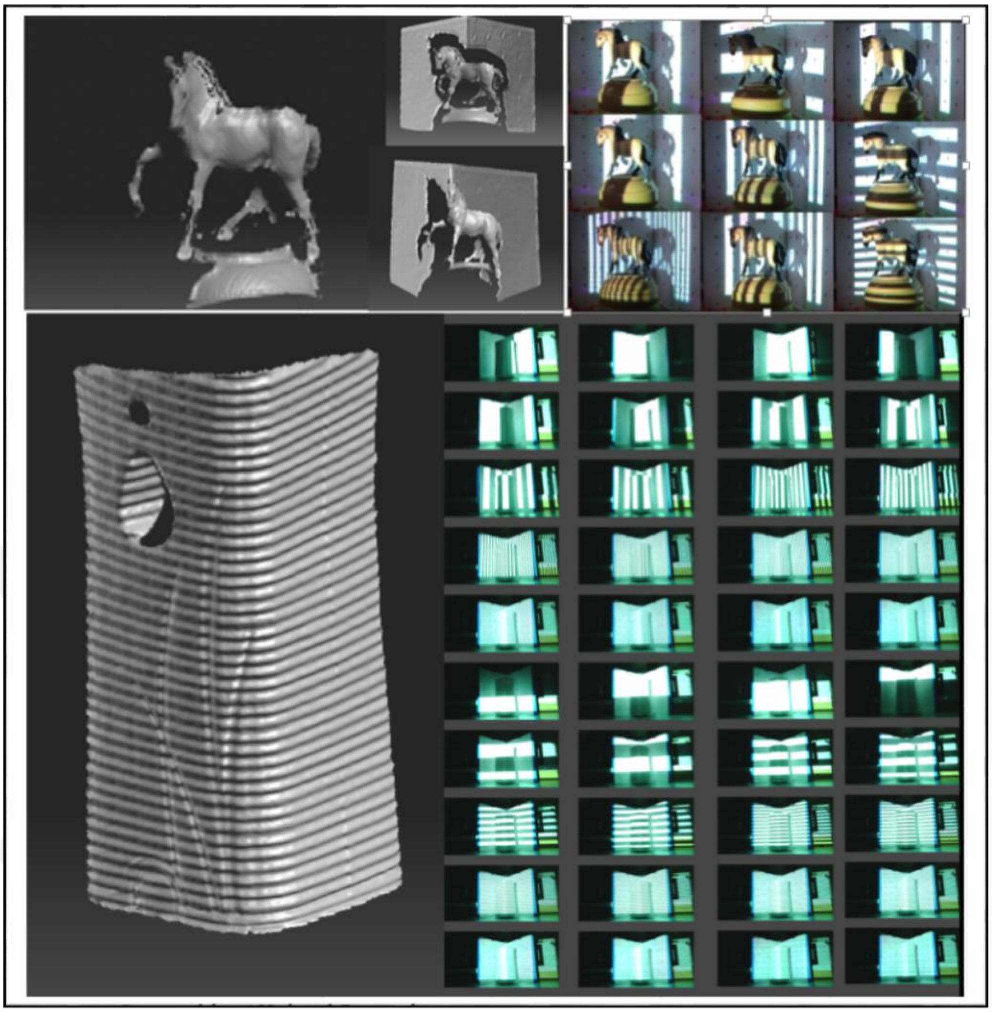

6.3 COMPARISON

Quality measurement can be decided by observation, but the time and distance required for the scanning process to deliver the intended outcome are essential parameters. To compare the two techniques we are required to prepare an ideal environment for the projector and the camera. We used a dark room without any kind of ambient light, then we selected an object with a mat surface to avoid light reflection as much as possible, and we aligned the camera with the projector.

6.3.1 Examining Binary Coded Patterns

Starting with binary coded pattern technique, we set a distance of 45*cm* between the object and the camera and then we acquired the result and we repeated the process with 60 *cm*, 120 *cm*, 250 *cm*, and 350 *cm*. The results are given in figure 6.8. As we can see in our results, the best range of distance is between 45*cm* and 120*cm*. When the distance exceeded 300 *cm*, the 3D image became distorted and unobservable. The time period required to capture and deliver an outcome with binary coded patterns is 13.7 seconds (±0.5 second).

Figure 0.8: Scanning Quality of Binary Coded Patterns Technique at Different Distance.

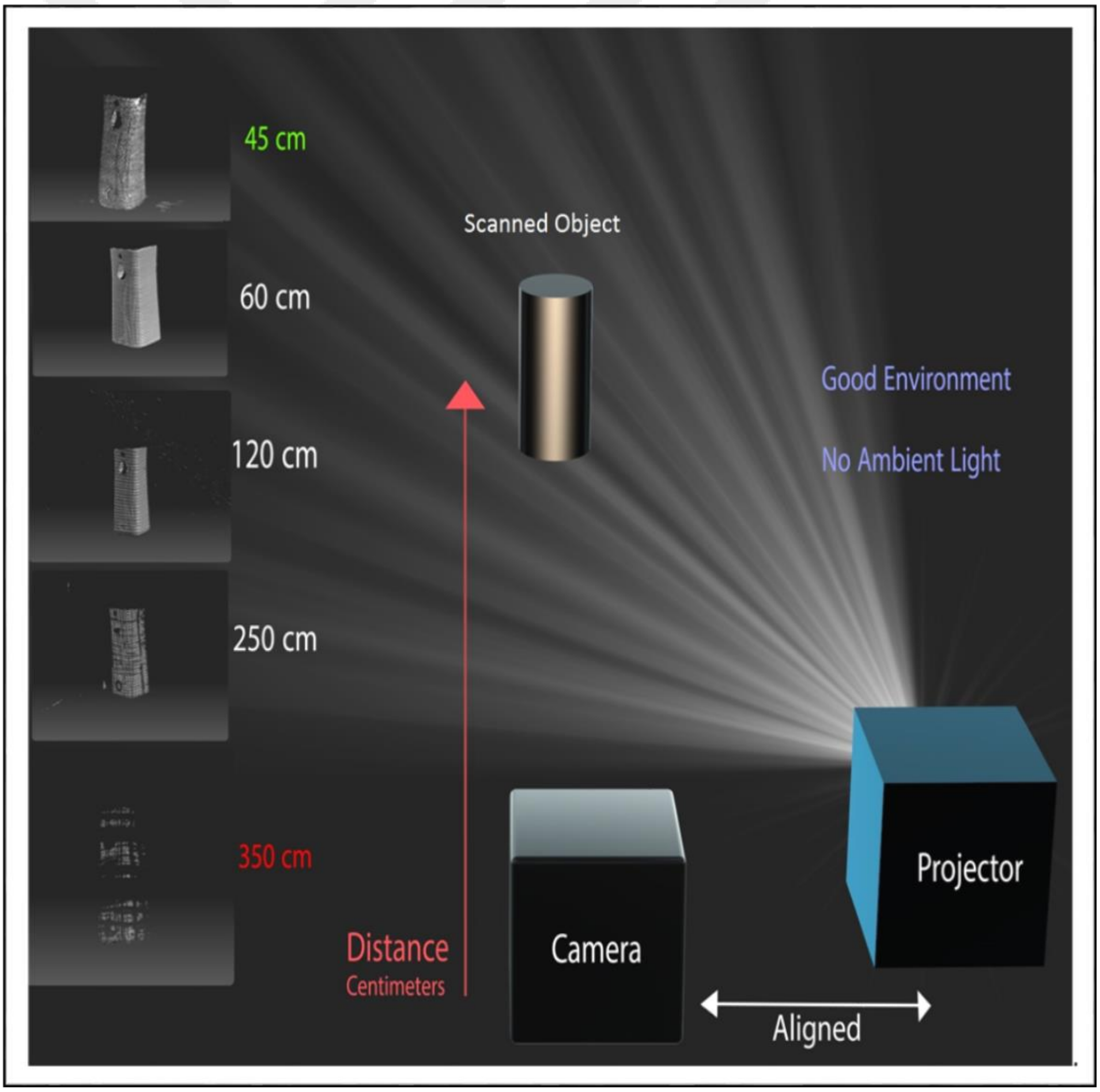

6.3.2 Examining Phase-Shifting Patterns

By using the same object and the same starting distance of 45cm, we began the same process as we did with binary coded patterns in the same environment. We were able to exceed the distance limit, at 350*cm* we had a good result and we kept extending the distance until the 3D image started deforming in 650*cm*. If we take a look at figure 6.9 we will see that in the short distance between 45*cm* and 60*cm* the 3D image has less quality than we had using binary coded patterns, but phase-shifting patterns quality in a range of 60*cm* and 600*cm* is better. The time required to accomplish capturing and processing the three 2D images and convert them to a 3D model is 2.8 seconds (±0.3 second).

Figure 0.9: Scanning Quality of Phase-Shifting Technique at Different Distance.

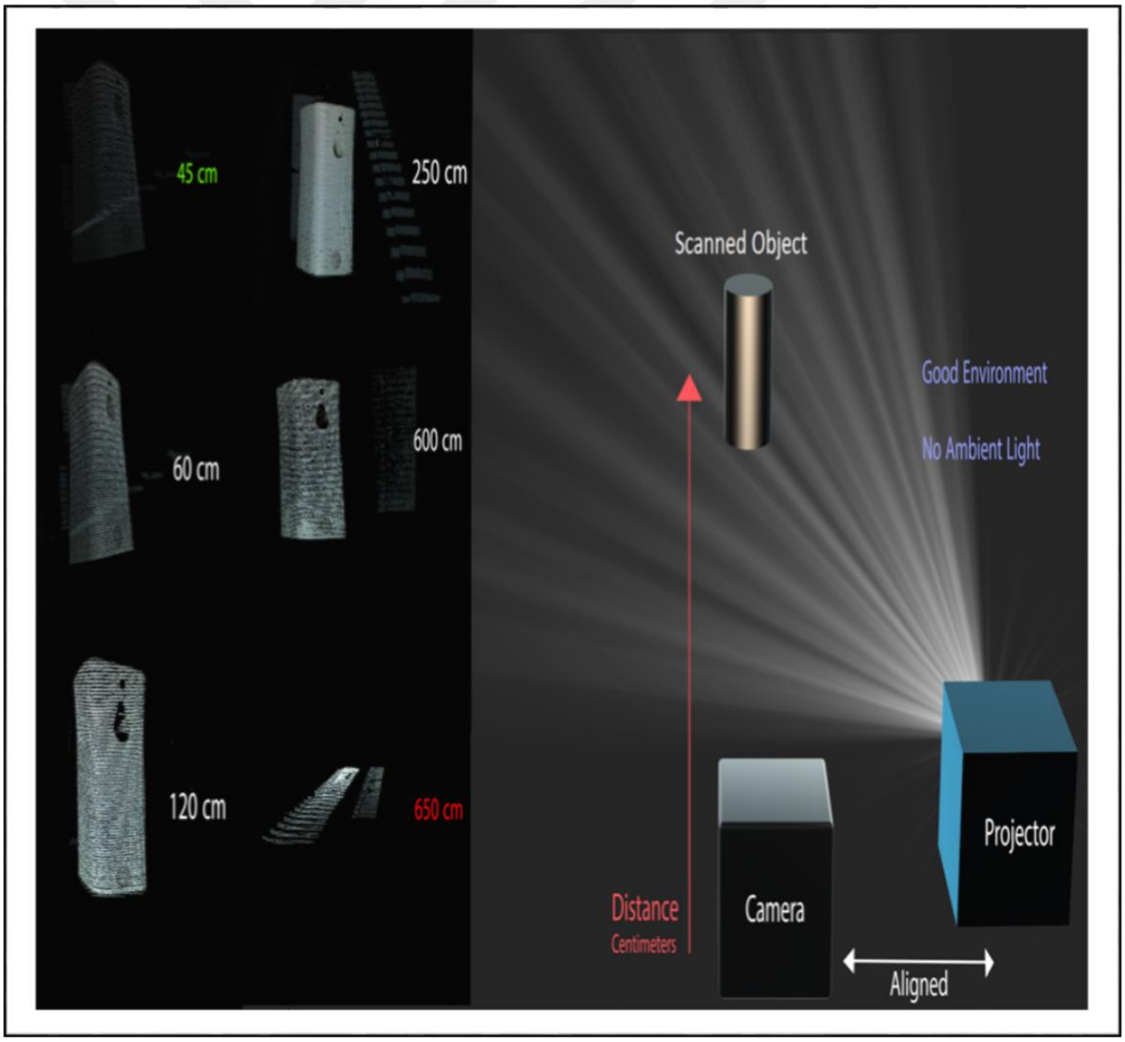

7. CONCLUSION

We provided a tight specification for most of the techniques used now days in 3D imaging systems. The reason for many methods is because each one has its own pros and cons and it is not possible to use one technique in all required applications. That has been said, the 3D imaging technologies have yet a large capacity to develop and improve more than 2D imaging systems. “Structured light scanner” is a phrase given to 3D scanner systems that require sweeping light (laser or light illuminations) on the targeted object. The difference between laser projection technique and light projection technique is that the first requires sweeping laser on the entire surface in order for the sensors to capture the geographic exterior of the object, while light projection scanner technique can be accomplished by illuminating the entire surface of the object all at once and process the required information from the 2D image. As the laser does not be affected by surrounding illumination lights or the projection distance, its intensity remains high throughout the scanning process. Thus Laser projection technique profits in occupying higher detailed results more than light projection methods. Light projection techniques in appropriate environment can offer high quality results as well, plus it can be accomplished in a shorter amount of time.

We chose to implement a phase-shifting and binary coded pattern technique because they have the advantages regarding the reliability, simplicity, cost, and accuracy, although the targeted object must stay static during the process of capturing patterns images by the optical sensors in both techniques, but the time requirement differs. The result was promising and highly satisfying in both systems. They share the same disadvantage of being a structured light 3D scanning systems using projector illumination, which make them vulnerable to the environmental light illumination and the distance of the projector from the targeted object. As the illumination intensity of the projection decreases more as it projects to a further distance, thus the projected patterns will lose resolution. And this issue is more intense in gray coded binary patterns. We concluded that as we project more patterns onto the surface of the object, it becomes harder to capture those patterns with the optical sensors, no matter how accurate is the camera or the quality of the projected light, the resolution limits of the projector can never be high enough to project as many patterns as we want. This limit bounds the resolution and the amount of details of the resulted 3D model to a certain range. As for phase-shifting technique, the pre-blurred patterns solve the issue of the distance limit. Pre-blurred patterns will remain blurred as the scene moves away from the projector. We used three images with phase-shifting patterns as the location of the strips moves down in each image, allowing us to cover the surface of the subject with required strips. The main downside of this technique remains in the details that can capture during the scanning process. If we take a look back at the facial scanned image in figure 6.3 we will notice some distance between the horizontal pixels. This issue accrued because the details of the gray color shifting from black to white can be distorted by the quality of the projected light. In other words, to obtain better results from the scanning process it requires a better projector with high light intensity, same goes for the camera resolution. But if we compare it to the 3D model in figure 6.7 which obtained by using binary coded patterns, we will see the least amount of distortion and distance between the pixels, because in binary coded patterns we used 41 different patterns and we started with black image and then white, doing so will deny any distortion in the 3D model. For example, if we project only white pattern on the surface of an object, during the process the black pixels, for example, in the captured images will mislead the system to process it as a pixel of a black strip, which will distort the 3D model. And as we mentioned, the projected strips will be blurred as the scene moves away from the projector. Thus, using the binary coded pattern method will suffer from this problem further than phase-shifting technique. In conclusion, using Phase-shifting patterns will benefit us in long distance and faster time process. Allowing us to scan human body parts in a short amount of time if they remain static. Binary coded patterns have the advantage of significantly higher quality of the scanning process and more detailed 3D model. But in cost of longer process time and shorter distance and being unable to capture dynamic objects. In conclusion, we determined that the advantages of using phase-shifting patterns outnumbers those of binary coded patterns for the following reasons:

1. Phase-shifting patterns much less period of time to capture images and process them.
2. The distortion caused by blurry patterns resulted by distance or manufacturing quality of the projector has less impact on the outcome of using phase-shifting patters.

3. Phase-shifting patterns requires much less images of the object to process and offer a 3D model. Thus, in some applications the memory capacity for the captured images is limited and can be a major issue if the system requires scanning multiple objects.
4. Phase-shifting technique does not demand high quality images in order to offer good results. This affects the costs of the equipment required for the system, such as the camera and the projector.

Using structured light 3D scanning now days in a verity of applications will draw the attention of younger researchers as there are numerous opportunities to develop it to the next era of technology.

REFERENCES

Books

Moigne, J. L., & Waxman, A. M. (1985). *Multi-resolution grid patterns for building range maps.* Dearborn: Society of Manufacturing Engineers.

Sagan, H. (1994). *Space Filling Curves,* Universitext Edition. New York: Springer.

Other Publications

Akca, D. (2011). Mediterranean Arhaeology and Archaeometry. 3D Modeling Of Cultural Heritage Objects, 12, pp 139-152.

Basri, & Jacobs. (2006). Photometric stereo with general, unknown lighting. International Journal of Computer Vision, 72, pp 239-257.

Boyer, K., & Kak, A. (1987). Color-encoded structured light for rapid active. Robot Vision Laboratory, pp 14 - 28.

Desjardins, D., & Payeur, P. (2007). Computer and Robot Vision. Dense Stereo Range Sensing with Marching Pseudo-Random Patterns, 3, pp 216 - 226.

Fredricksen, H. (1982, April). SIAM Review. A survey of full length nonlinear shift register cycle, 24, pp 195-221.

G. Durdle, J. Thayyoor, & J. Raso. (1998). Electrical and Computer Engineering. An improved structured light technique for surface reconstruction of the human trunk, 2, pp 874 - 877.

Geng, J. (2011). Advances in Optics and Photonics. Structured-light 3D surface imaging: a tutorial, 3(2), pp 128-160.

Geng, J. (2011). Structured-light 3D surface imaging:. Advances in Optics and Photonics, 3, pp 138-140.

Griffin, P., Narasimhan, L. S., & Yee, S. R. (1992, June). Pattern Recognition. Generation of uniquely encoded light patterns for range data acquisition, 25(6), pp 609-616.

Heike, L., Upson, K., Stuhaug, E., & Weinberg, M. (2010, July 28). 3D digital stereophotogrammetry: a practical guide to facial image acquisition. Retrieved from Head & Face Medicine: http://www.head-face-med.com/content/6/1/18

Ishii, I. (2015, November 20). A Coded Structured Light Projection Method for. Retrieved from intechopen: http://cdn.intechopen.com/pdfs-wm/32185.pdf

Ishii, I. (2012). A Coded Structured Light Projection Method for High-Frame-Rate 3D Image Acquisition [online], Hiroshima University, http://cdn.intechopen.com/pdfs-wm/32185.pdf

L. Zhang, B. Curless, & M. Seitz. (2002). 3D Data Processing Visualization and Transmission. Rapid Shape Acquisition Using Color Structured Light, 24 - 36.

M. Maruyama, & S. Abe. (1993). “Range sensing by projecting multiple slits. IEEE.

MacWilliams, F., & Sloane, N. (1976). Proceedings of the IEEE. Pseudo-random sequences and arrays, 12(64), pp 1715 - 1729.

Maruyama, M., & Abe, S. (199Pattern Analysis and Machine Intelligence. Range sensing by projecting multiple slits, pp 647 - 651.

Moigne, J. L., & Waxman, A. M. (1985). Multi-resolution grid patterns for building range maps. Dearborn: Society of Manufacturing Engineers.

Pajdla, T. (1995). Bcrf—binary-coded illumination range finder reimplementation. Leuven: Technical Report KUL/ESAT/MI2/9502.

Rusted, J. (2013, November 17). Accident Investigation Background. Retrieved from geosystems: http://psg.leica-geosystems.us/page/applications/crash-investigations/

Rusted, J. (2013). Accident Investigation Background. Retrieved from geosystems: http://psg.leica-geosystems.us/page/applications/crash-investigations/

Woodham. (1989). Shape from shading. Photometric method for determining surface orientation from multiple images, pp 513-531.